DTIC FILE COPY

(2)

USAAVSCOM TM-87-D-5

US ARMY
AVIATION
SYSTEMS COMMAND

TEST OF AN 0.8-SCALE MODEL OF THE AH-64 APACHE IN THE NASA LANGLEY FULL-SCALE WIND TUNNEL

AD-A196 129

Frederick A. Raitch

May 1988

DTIC
ELECTE
JUL 0 6 1988
S D
H

Approved for public release;
distribution is unlimited.

AVIATION APPLIED TECHNOLOGY DIRECTORATE
US ARMY AVIATION RESEARCH AND TECHNOLOGY ACTIVITY (AVSCOM)
Fort Eustis, VA. 23604-5577

88 6 [illegible] 061

DISCLAIMERS

The findings in this report are not to be construed as an official Department of the Army position unless so designated by other authorized documents.

When Government drawings, specifications, or other data are used for any purpose other than in connection with a definitely related Government procurement operation, the United States Government thereby incurs no responsibility nor any obligation whatsoever; and the fact that the Government may have formulated, furnished, or in any way supplied the said drawings, specifications, or other data is not to be regarded by implication or otherwise as in any manner licensing the holder or any other person or corporation, or conveying any rights or permission, to manufacture, use, or sell any patented invention that may in any way be related thereto.

UNCLASSIFIED

SECURITY CLASSIFICATION OF THIS PAGE

REPORT DOCUMENTATION PAGE

1a. REPORT SECURITY CLASSIFICATION Unclassified	1b. RESTRICTIVE MARKINGS
2a. SECURITY CLASSIFICATION AUTHORITY 2b. DECLASSIFICATION / DOWNGRADING SCHEDULE	3. DISTRIBUTION / AVAILABILITY OF REPORT Approved for public release; distribution is unlimited.
4. PERFORMING ORGANIZATION REPORT NUMBER(S) USAAVSCOM TM 87-D-5	5. MONITORING ORGANIZATION REPORT NUMBER(S)
6a. NAME OF PERFORMING ORGANIZATION Aviation Applied Technology Directorate 6b. OFFICE SYMBOL *(If applicable)*	7a. NAME OF MONITORING ORGANIZATION
6c. ADDRESS *(City, State, and ZIP Code)* U.S. Army Aviation Research and Technology Activity (AVSCOM) Fort Eustis, VA 23604-5577	7b. ADDRESS *(City, State, and ZIP Code)*
8a. NAME OF FUNDING / SPONSORING ORGANIZATION 8b. OFFICE SYMBOL *(If applicable)*	9. PROCUREMENT INSTRUMENT IDENTIFICATION NUMBER
8c. ADDRESS *(City, State, and ZIP Code)*	10. SOURCE OF FUNDING NUMBERS PROGRAM ELEMENT NO. / PROJECT NO. / TASK NO. 80-06 / WORK UNIT ACCESSION NO.

11. TITLE *(Include Security Classification)*

Test of an 0.8-Scale Model of the AH-64 Apache in the NASA Langley Full-Scale Wind Tunnel

12. PERSONAL AUTHOR(S)

Frederick A. Raitch

13a. TYPE OF REPORT	13b. TIME COVERED	14. DATE OF REPORT *(Year, Month, Day)*	15. PAGE COUNT
Memorandum	FROM _____ TO _____	May 1988	42

16. SUPPLEMENTARY NOTATION

17. COSATI CODES			18. SUBJECT TERMS *(Continue on reverse if necessary and identify by block number)*	
FIELD	GROUP	SUB-GROUP	Wind tunnel	Pylon
			AH-64 Apache	Fuselage
			Hub	Pressure distributions

19. ABSTRACT *(Continue on reverse if necessary and identify by block number)*

This document summarizes the tests of an 0.8-scale model of the upper half of the AH-64 air vehicle in the NASA Langley full-scale tunnel, primarily to determine the large-scale blockage effects discovered during earlier tests of the same model in the NASA Langley 4- by 7-meter tunnel. As background information, and to provide continuity, the earlier program is outlined. The models were large and heavy, and therefore the balances had large capabilities. Yet, because of operational limitations with both wind tunnels involved, the only data that overlapped in "flight" conditions were at very low velocities. Thus, the results of these tests were inconclusive due to the time-honored difficulty of small differences in large numbers. This effect carried over into other, auxiliary tests performed during the same test series, each concerned with an attempt to detect small differences.

20. DISTRIBUTION / AVAILABILITY OF ABSTRACT ☒ UNCLASSIFIED/UNLIMITED ☐ SAME AS RPT. ☐ DTIC USERS	21. ABSTRACT SECURITY CLASSIFICATION Unclassified
22a. NAME OF RESPONSIBLE INDIVIDUAL F. Raitch	22b. TELEPHONE *(Include Area Code)* (804) 878-4371 22c. OFFICE SYMBOL SAVRT-TY-ATA

DD FORM 1473, 84 MAR

83 APR edition may be used until exhausted.
All other editions are obsolete.

SECURITY CLASSIFICATION OF THIS PAGE

UNCLASSIFIED

SUMMARY

This report summarizes tests on an AH-64 air vehicle in the NASA Langley full-scale tunnel during the summer of 1982. The purpose of these tests was to determine the large-scale blockage effects discovered during earlier tests beginning in the late 1970s of the same model in the NASA Langley 4- by 7-meter tunnel. Both programs are outlined in the document.

The models were large and heavy, and therefore the balances had large capabilities. Yet, because of operational limitations with both wind tunnels involved, the only data that overlapped in "flight" conditions were at very low velocities. Thus, the results of these tests were inconclusive due to the time-honored difficulty of small differences in large numbers. This effect carried over into other, auxiliary tests performed during the same test series, each concerned with an attempt to detect small differences.

2
F

DTIC
COPY
SPECTED
6

Accession For
NTIS GRA&I ☑
DTIC TAB ☐
Unannounced ☐
Justification

By
Distribution/
Availability Codes
Dist | Avail and/or Special
A-1

TABLE OF CONTENTS

	Page
SUMMARY	iii
LIST OF FIGURES	vi
LIST OF TABLES	viii
WIND TUNNEL TESTS OF LARGE- AND SMALL-SCALE ROTOR HUBS AND PYLONS	1
Background	1
Description of the Wind Tunnel	2
Test Models	2
Test Devices	4
Generalized Rotor Model System (GRMS)	4
Hub and Pylon Evaluation Rig (HPER)	6
Instrumentation	7
Computer Analysis	10
NASA Langley 4- by 7-Meter Tests	12
Procedure	12
Results	13
Summary of Findings	23
CORRECTIVE MEASURES PRIOR TO FULL-SCALE TUNNEL TESTS	27
HPER TESTS IN FULL-SCALE WIND TUNNEL	28
Matrix of Test Variables	28
General Instrumentation Problems	31
Analysis of Results	33
Blockage	33
Effects of New Mast Inlet Design	36
Strakes	36
Pylon Drag	36
Effect of Fan Thrust on Pylon Pitching Moment	38
Duct Losses	39
Drag of the Alternate Exhaust Ducts	39
Summary of Findings	41
BIBLIOGRAPHY	42

LIST OF FIGURES

Figure		Page
1	GRMS in 4- by 7-meter tunnel	3
2	HPER in 4- by 7-meter tunnel	4
3	GRMS mechanism in an earlier model helicopter	5
4	GRMS details	5
5	GRMS main rotor hub details	6
6	HPER foundation frame	7
7	HPER hub rotation unit	8
8	HPER balances in place in the foundation frame	8
9	HPER details	9
10	GRMS paneling used in computer analysis	11
11	HPER paneling used in computer analysis	12
12	HPER hub and pylon drag reduction due to hub fairing	14
13	GRMS hub and pylon drag reduction due to hub fairing	16
14	Effect of Reynolds number on pylon parasite drag	19
15	Effect of mast inlet mass flow on pylon parasite drag	19
16	Effect of Reynolds number on hub drag	21
17	Effect of Reynolds number on fuselage drag (GRMS)	22
18	Effect of hub rotation on HPER hub drag	24
19	Effect of hub rotation on GRMS hub drag	25
20	HPER model in full-scale tunnel	29
21	Full-scale tunnel drive unit servicing	30
22	Blockage corrections applied to HPER data from NASA Langley 4- by 7-meter wind tunnel along Buttline 5	34
23	Blockage corrections applied to HPER data from NASA Langley 4- by 7-meter wind tunnel along Waterline 132	34

LIST OF FIGURES (Continued)

Figure		Page
24	Fuselage surface pressure coefficient data from HPER tests in NASA Langley full-scale tunnel along Buttline 5 compared to similar data from tests in NASA Langley 4- by 7-meter tunnel	35
25	Fuselage surface pressure coefficient data from HPER tests in NASA Langley full-scale tunnel along Waterline 132 compared to similar data from tests in NASA Langley 4- by 7-meter tunnel	35
26	New mast inlet data	37
27	Fan thrust via balance vs pressure rakes	40

LIST OF TABLES

Table		Page
1	Dynamic conditions obtained in the 4- by 7-meter tunnel	13
2	Drag buildup by component	13
3	Drag increments due to airframe modifications	17
4	Dynamic conditions obtained in the full-scale tunnel	28
5	Variables in full-scale tunnel tests	31
6	Typical matrix of test data points	32
7	Effect of tunnel dynamic pressure on fan thrust	38
8	Drag of alternate exhaust ducts	39

WIND TUNNEL TESTS OF LARGE- AND SMALL-SCALE ROTOR HUBS AND PYLONS

BACKGROUND

In the late 1970s, cooperation and coordination between the U.S. Army Aviation Materiel Laboratories,* the David Taylor Model Basin,** and NASA Langley Research Center led to development of a Comprehensive Drag Plan in which helicopter aerodynamic drag items would be studied in an orderly, systematic manner. Early plans called for an array of models representing a generic cargo/utility type helicopter and a generic gunship type helicopter. Models to two different scales were to be constructed and fitted to two available test rigs - the NASA Generalized Rotor Model System (GRMS) and the Navy Hub and Pylon Evaluation Rig (HPER). Computer programs studying the aerodynamics of bluff bodies were in a formative period at the time, but it was felt that one or two programs were well-enough developed to augment the experimental drag studies.

While this program was in its initial phases, the AH-64 Apache and other helicopter development programs were encountering aerodynamic problems involving main rotor wake, hub and pylon disturbances, and airflow through and around the nacelles, described as follows:

1. In some flight regimes, the engines of some helicopters were experiencing inlet disturbances which led to loss of power of sufficient degree to cause concern. Air transportability had dictated low main rotor placement, which was suspect in contributing to this, but existing data was insufficient to determine a solution to the problems.

2. During developmental flight tests, the AH-64 Apache experienced disturbing random motion on weapons firing runs, attributed to turbulent airflow from the hub and pylon region striking the tail surfaces. It was thought that fairing part of the main rotor hub, improving the fairing around the main rotor shaft, and adding strakes down the back of the fuselage between the engines could help improve the airflow characteristics enough to ease this random motion of the vehicle.

3. Also on the AH-64 Apache, the air mass flow for transmission cooling, engine cooling, and exhaust dilution was insufficient in some flight regimes and generally produced unstable inlet pressures in nearly all flight regimes. It was thought that this was partly due to the inlet location being submerged in the area of the main rotor shaft and hub, and alternative inlet configurations were being studied.

The cooperative interagency drag program was converted from "generic" to "specific" in order to respond to these problems.

*Now the Aviation Applied Technology Directorate (AATD).
**Now the David W. Taylor Naval Ship Research and Development Center.

By the time this program was under way, the Navy interest had been diverted to projects of more immediate Navy requirements, but they continued to offer their assistance in the loan of test hardware. AATD and NASA Langley continued the program, which involved wind tunnel testing combined with computer analysis, with NASA Langley providing the VSTOL tunnel (now called the 4- by 7-meter tunnel). Hughes Helicopters (now McDonnell Douglas Helicopter Company) and Analytical Methods, Incorporated (AMI) were placed under contract to perform the computer analysis, build the models, oversee the tunnel tests, and write the report (see Reference 1).

DESCRIPTION OF THE WIND TUNNEL

The NASA Langley 4- by 7-meter tunnel has a design maximum velocity of approximately 200 knots. At the time these tests were performed, the minimum velocity for smooth flow was approximately 60 knots, limited by flow separation and turbulence. This limit had a severe impact on the data comparisons with later tests. The test section is equipped with a boundary-layer removal system on the floor ahead of the model, which helped somewhat. (Since these tests, aerodynamic improvements in the tunnel have considerably lowered the minimum velocity at which smooth flow can be achieved in the test section.)

TEST MODELS

The problems to be examined in this effort were heavily dependent upon two factors: realistic Reynolds number and realistic main rotor wake. Experimental investigation of some of the problems, especially those occurring at low speed, required at least a partial representation of the main rotor wake, which implied a rather small model, while adequate Reynolds number (and thus as large a model as feasible) was of prime importance in the investigation of problems influenced by factors other than main rotor wake. In addition, the effects of main rotor wake are difficult to scale under any circumstances, but especially in the vicinity of the hub and pylon, and in the inlets, coolers, and internal airflow regions.

NASA had available a test device which could mount a model approximately 0.3 scale and could spin a 10.5-foot-diameter main rotor loaded appropriately to simulate the AH-64 Apache system. In designing a larger model, a full scale was considered but was set aside as not feasible nor necessary. In-flight tuft studies on the prototype showed that the flow along Waterline 104 was straight and stable in cruise flight. This meant that the model could be truncated at this level for overall size reduction without adversely affecting the flow over the remaining portion of the model. The wind tunnel staff estimated that even this truncated model would be large enough to cause excessive blockage, so 0.8 scale was selected as a reasonable compromise.

[1]Logan, A.H., Prouty, R.U., and Clark, D.R., Wind Tunnel Tests of Large- and Small-Scale Rotor Hubs and Pylons, USAAVRADCOM TR 80-D-21, Applied Technology Laboratory, U.S. Army Research and Technology Laboratories (AVRADCOM), Fort Eustis, Virginia, April 1981, AD A098510.

Thus, two different models to two different scales were involved in the testing: a 0.30 scale model of the fuselage and wing, with main rotor (see Figure 1) and an 0.80 scale model of the upper half of the fuselage, with rotor hub only (see Figure 2). Neither of the models was equipped with a tail rotor, as this was not pertinent to the problems being examined.

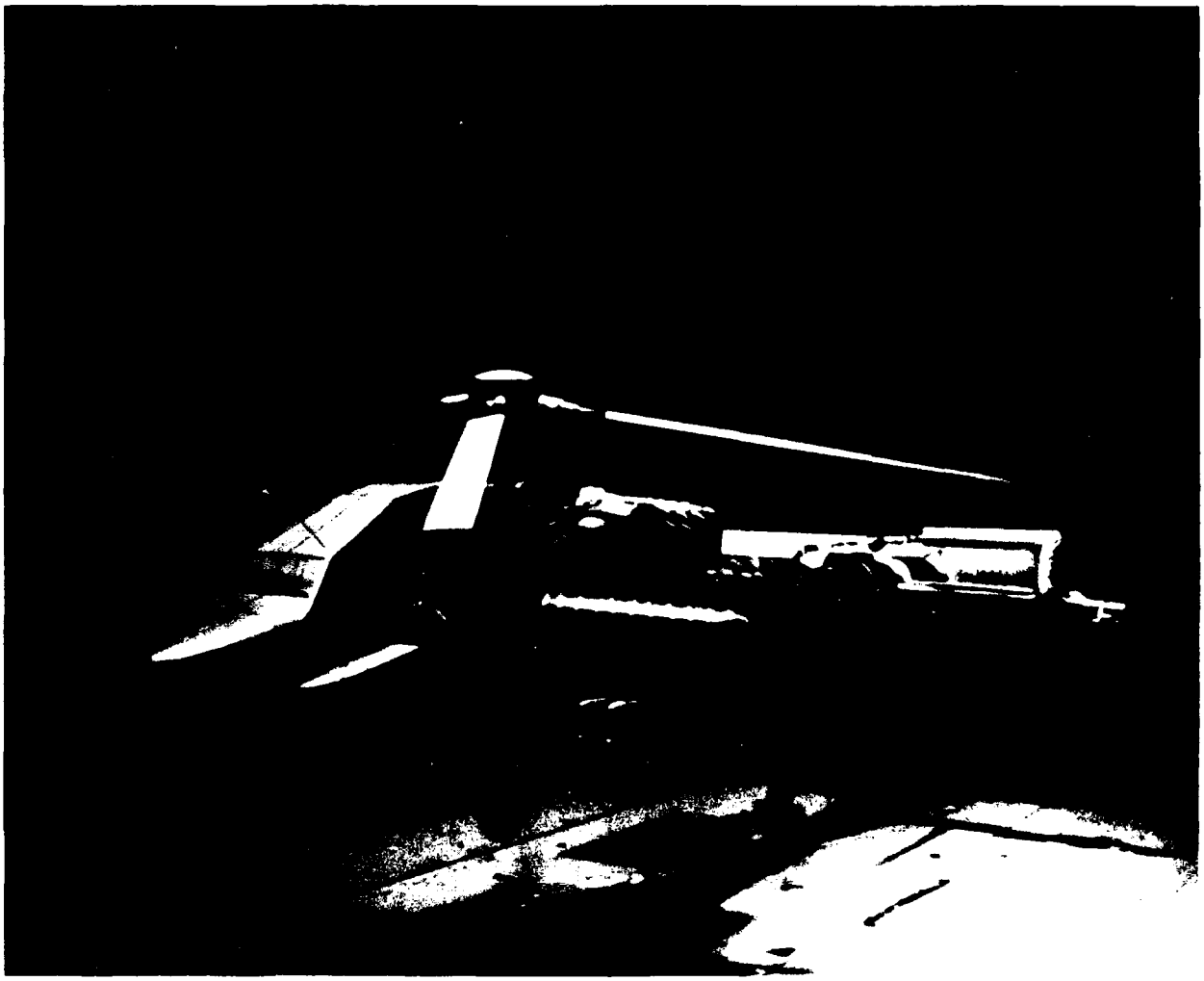

Figure 1. GRMS in 4- by 7-meter tunnel.

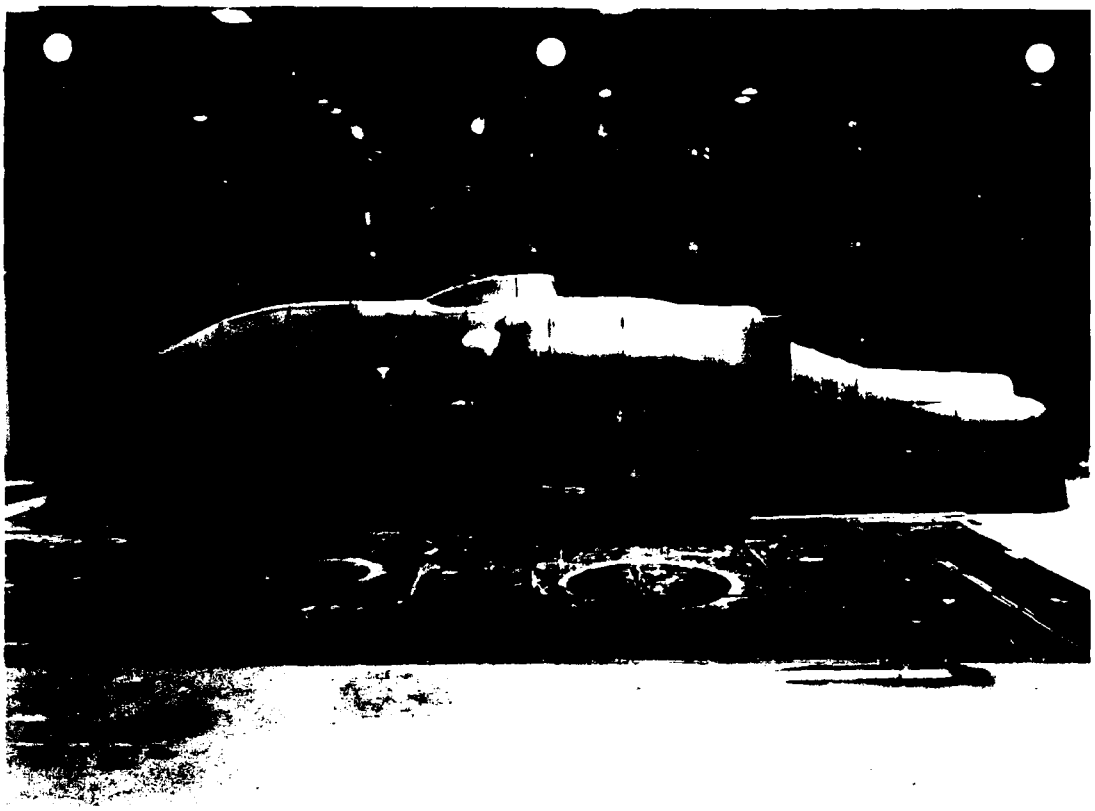

Figure 2. HPER in 4- by 7-meter tunnel.

TEST DEVICES

Generalized Rotor Model System (GRMS)

The GRMS was a test device tailored for the Nasa Langley 4- by 7-meter wind tunnel. Figure 3 shows the GRMS (inside an earlier configuation) with the shell of the model partially removed. The GRMS was mounted in the tunnel on a special sting (partially shown in Figure 4), which provided angular placement within a 60-degree cone while keeping the model in the center of the tunnel. Two water-cooled electric motors geared together turned a 10.5-foot-diameter main rotor. The articulated rotor hub was equipped with cyclic and collective pitch controlled remotely during the tests, as shown in Figure 5. The shell of the model was fitted with 3-inch-diameter air-driven fans to simulate inlet and exhaust flow. Because of the width of the machinery and the narrowness of the prototype AH-64 Apache fuselage, the model fuselage scale had to be 0.30. The maximum main rotor that could be spun by the machinery was 10.5 feet, which resulted in the main rotor scale coming out to be 0.21. This combination of model shell and test machinery resulted in a hybrid test device, which was nonetheless acceptable for the planned tests, since the main rotor wake on this model was needed only to provide a realistic disturbance in the flow field of the hub and pylon region, involving only about the inner third of the main rotor wake (see Figure 4). This device is described in Reference 1.

Figure 3. GRMS mechanism in an earlier model helicopter.

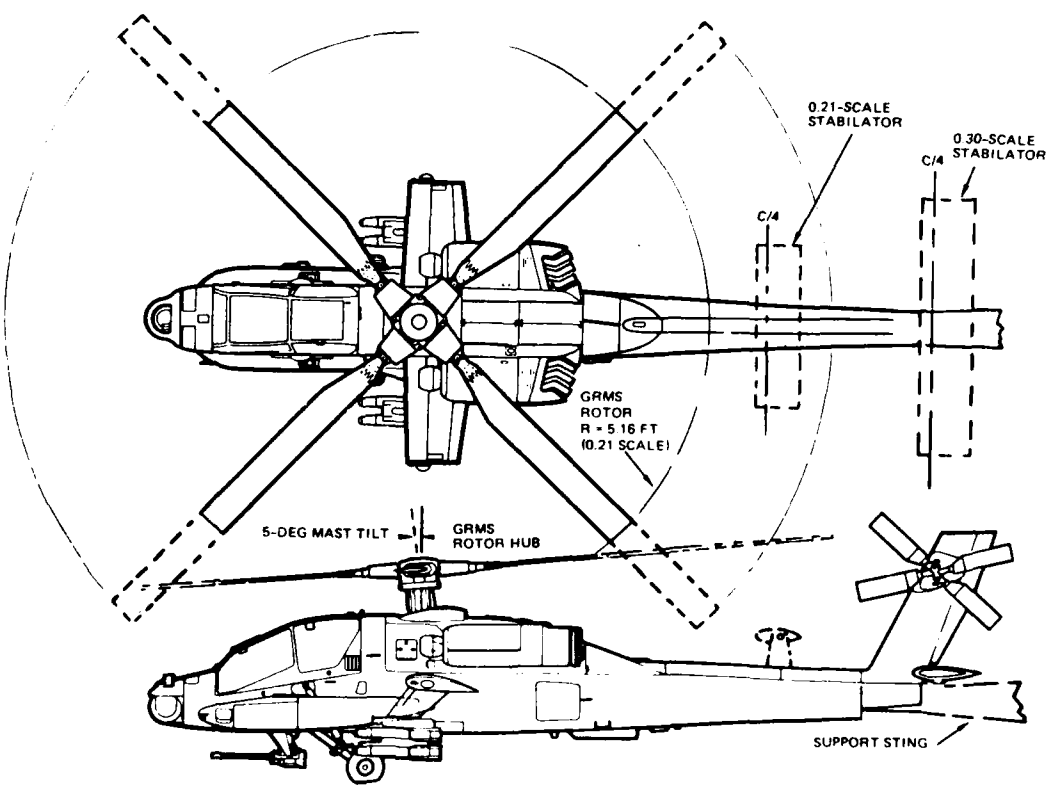

Figure 4. GRMS details.

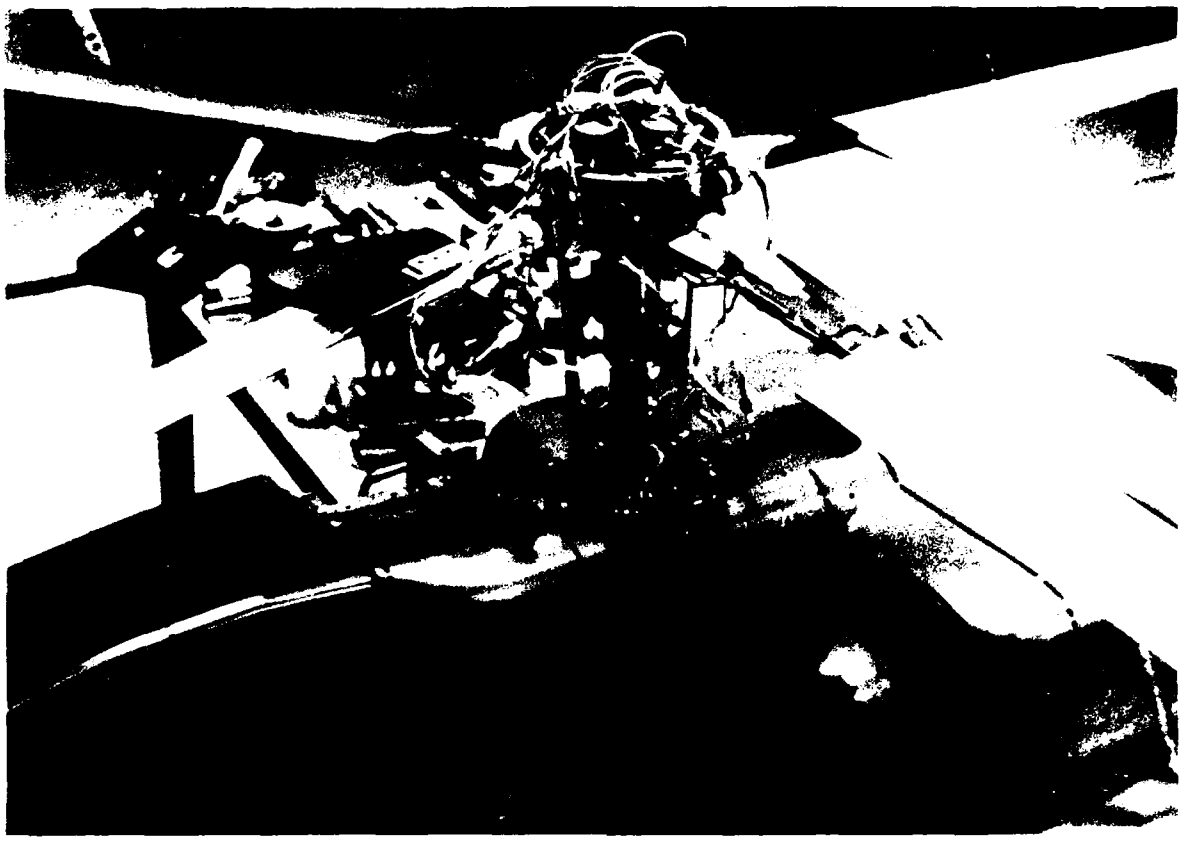

Figure 5. GRMS main rotor hub details.

Hub and Pylon Evaluation Rig (HPER)

The David W. Taylor Naval Ship Research and Development Center possessed a test rig called the Hub and Pylon Evaluation Rig (HPER), to which a large-scale model shell of the AH-64 could be fitted (as shown in Figure 6) and which would provide instrumentation appropriate to these tests. This device was a complex of steel and aluminum I-beams and channels forming two nested frameworks: one forming the foundation for the entire mode and the other holding the outer skin of the model. Load cells between these two frameworks sensed the forces and moments on the model.

The test rig provided variable pitch angles for the main portion of the model, through a motor-driven screw jack and circular arc tracks (both visible in Figure 6) and a similar arrangement that provided variable pitch angle for the hub and main rotor. The original instrumentation was reasonably accurate, but the nested framework arrangement led to extraneous force and moment readings on the load cells due to thermal expansion and contraction of the two frameworks. This rig was borrowed from the Navy and delivered to NASA Langley, where it was modified to improve the instrumentation and add rotation to the main rotor shaft. The modified foundation is shown in Figure 6.

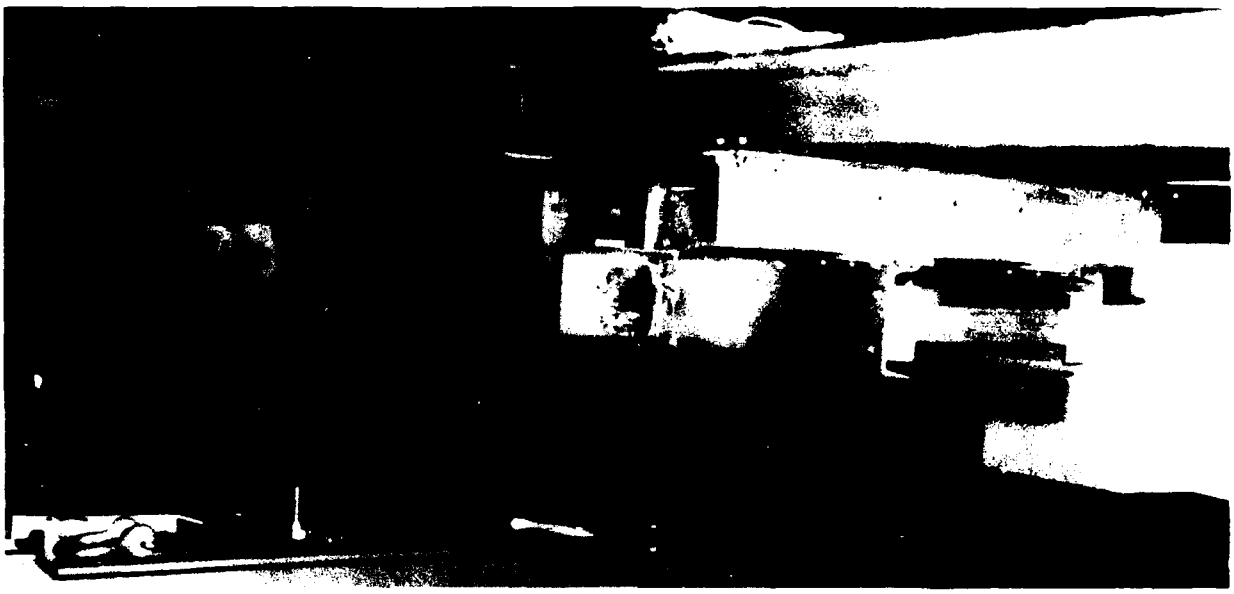

Figure 6. HPER foundation frame.

The original fixed hub configuration was modified to provide rotation using a hydraulic motor driving the rotor shaft through a 3-inch-wide toothed belt (see Figure 7). Hub rotation rate was sensed by an optical sensor reading a band of black and white marks on the rotor shaft, calibrated by a strobe system. This model and the smaller scale GRMS were equipped to simulate inlet and exhaust flow, and to measure surface pressures over the entire shape.

The modified rig incorporated two independent balance systems shown in Figure 8. The forward balance supported the upper portion of the fuselage. The aft balance supported the hub and hub drive mechanism.

The HPER model had freedom in pitch, which required geometry that would permit pitch changes without interfering with the floor. This required a windscreen to prevent airflow between the tunnel floor and the bottom of the fuselage shell shown attached to the test section floor in Figure 2.

Instrumentation

Figure 9 shows the portion of the AH-64 Apache represented in these tests. The dashed line indicates the prototype AH-64 Apache shape. The split line indicates the division between the instrumented and the noninstrumented portions of the model. The presence of the windscreen defined the lowest level on the side of the fuselage at which valid data could be obtained, namely Waterline 132, which corresponded to the initial location of the vortex sheet from the wing trailing edge, if the model had been equipped with the wing.

BL 5 is of particular interest, being along the top of the fuselage and nearly on the plane of symmetry. It is offset 5 inches from the plane of symmetry because of the plates joining the left and right halves of the model shell, and it is interrupted by the hub region.

Figure 7. HPER hub rotation unit.

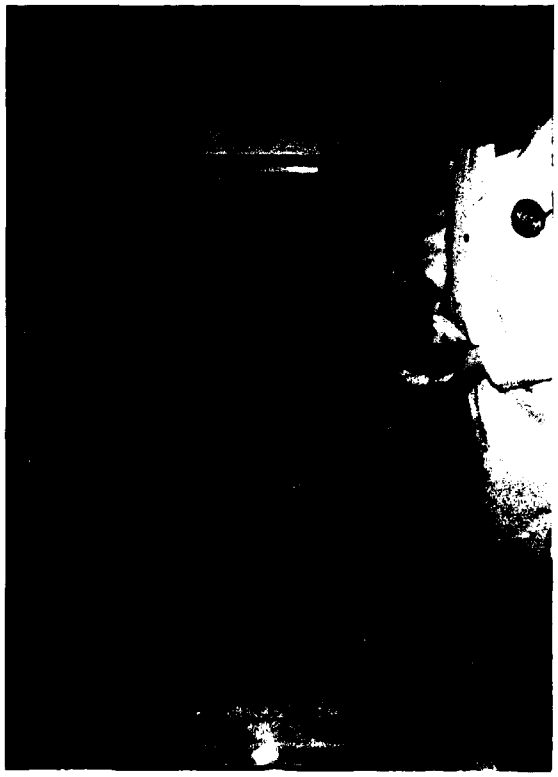

Figure 8. HPER balances in place in the foundation frame.

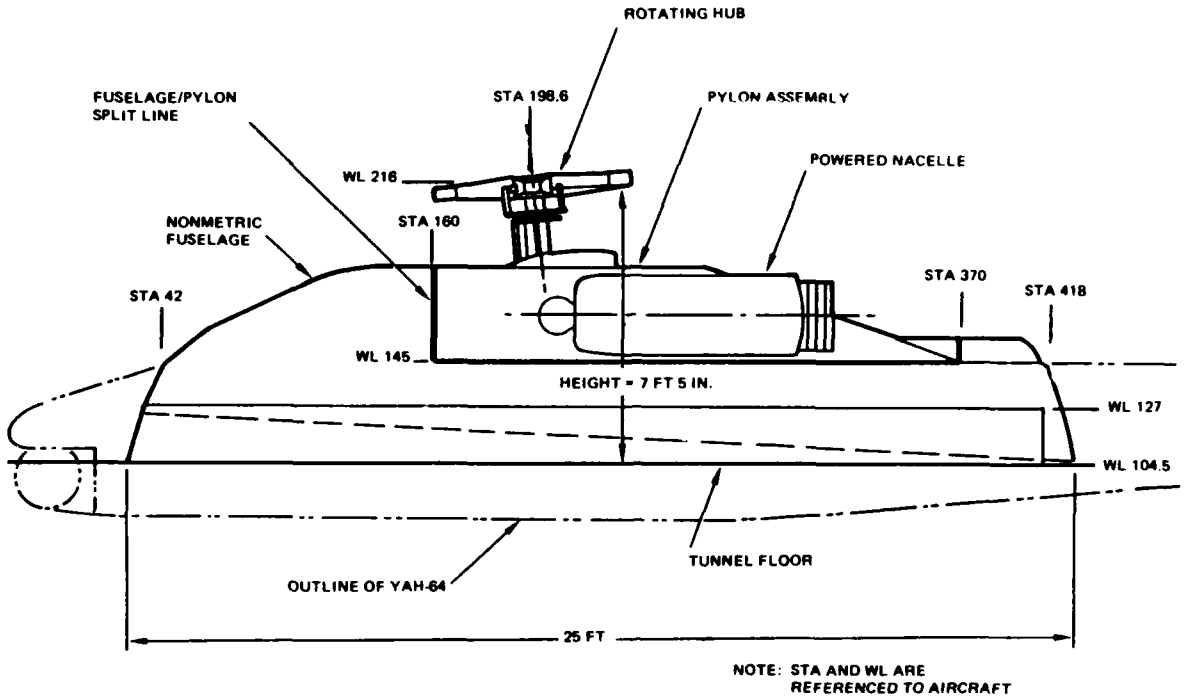

Figure 9. HPER details.

Both models were fitted to existing test rigs which held the shapes at the desired angle to the relative wind and provided main rotor rotation. The 0.3 scale model shell was fitted to the GRMS and the 0.8 scale model shell was fitted to the HPER. The models and test devices within them were instrumented similarly, with the following items being sensed:

1. Pylon longitudinal force
2. Pylon lateral force
3. Pylon normal force
4. Pylon rolling moment
5. Pylon pitching moment
6. Pylon yawing moment
7. Hub lateral force
8. Hub normal force
9. Hub rolling moment
10. Hub pitching moment
11. Hub yawing moment
12. Hub RPM
13. Hub angle of attack
14. Fan No. 1 dynamic pressure
15. Fan No. 2 dynamic pressure
16. Tunnel dynamic pressure
17. Fuselage surface pressures

Items 1 through 11 were measured by two balances (one for the pylon and one for the hub), precisely machined steel cylinders instrumented with strain gages.

Item 12 was sensed by an optical sensor reading the passage of alternating black and white marks on the hub shaft, electronically processed into RPM readings.

Item 13 was sensed by an inertial sensor mounted on the hub drive system frame, with direct digital readout in the control room.

Items 14 and 15 were sensed by fan duct pressure rakes mounted 8 inches downstream of each fan. These rakes were streamlined brass tubing with 3/4-inch chord mounted across the diameter of each fan exhaust duct. Each of these diametral tubes was pierced along the leading edge by twelve 1/16-inch brass tubes placed so that the pressure inside the streamlined tube became a measure of the dynamic pressure produced by the fan.

Item 16 was sensed by a conventional system already installed in the tunnel. This system is a number of carefully placed pitot tubes and static pressure ports.

Item 17 was sensed by five pressure transducers. Each was connected to 40 pressure ports on the surface of the fuselage model, through a scanning valve which let the transducer read each pressure in sequence, at approximately 1.2 readings per second.

COMPUTER ANALYSIS

It was felt that computer analysis techniques were sufficiently advanced to provide at least a guide to solutions, and to reduce the number and variety of costly wind tunnel tests. Thus, analytical computation was combined with wind tunnel test methods in an attempt to resolve the stated problems.

To serve the analytical computation requirements of this effort, a computer code was needed that could combine a panel model of the surface of the vehicle with a blade-element rotor wake model and could calculate the surface pressures and velocities on each panel with sufficient accuracy to permit integration of these pressures into total body forces, and to permit integration of these velocities into accurate descriptions of the behavior of streamlines along the vehicle. The aerodynamic computer code "VSAERO" fulfilled these requirements and was used to analyze pertinent configurations prior to wind tunnel tests.

The fuselage surfaces were described by the accepted paneling method, with the pressure being calculated at the control point located within each panel. The wind tunnel models were equipped with pressure sensors located to coincide with these mathematical control points. This permitted a direct overlay of surface pressures from calculation and from the wind tunnel models at two different scales.

In VSAERO, nonuniform inflow is accepted as input and regions of separated flow are determined by the program calculating velocity gradients that suggest that separation is about to occur. The effect of rotor downwash on the horizontal and vertical stabilizers can be determined, and also the effect of fuselage- and wing-induced upwash on rotor forces and moments. These features were especially useful, since the AH-64 Apache problems include all these elements. Fuselage panel computations and rotor blade element computations are run in series, with the connecting link being a panel model of the rotor disc and a time-averaged vortex model of the rotor wake. The rotor loads are fed as boundary conditions to the panel model which solves for the body forces, distorts the rotor wake in the presence of the fuselage, and feeds back to the rotor model an updated inflow distribution. The fuselage paneling used in the computerized analysis is illustrated in Figures 10 and 11.

The GRMS paneling took 423 panels and the HPER, 326 panels. In each case, a few panels were devoted to a representation of the wind tunnel walls, floor, and ceiling. The computer runs were made by AMI on the Control Data Corporation CYBER Series Computers at NASA Langley Analysis and Computation Division, from AMI's terminals in the Seattle area.

No attempt was made to model the detail in the hub, shaft, and control linkage area. Instead, an appropriate momentum model was developed based on the good correlation between hub frontal area and drag noted in Reference 2.

In the regions where the pressure gradient was of such a character as to make separation a possibility, the paneling was made more dense than in the surrounding areas.

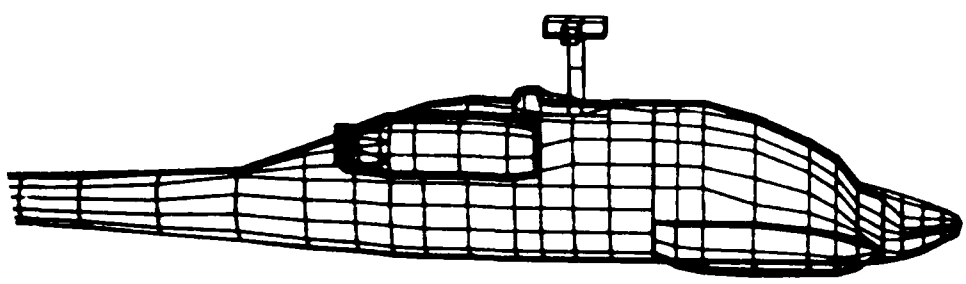

Figure 10. GRMS paneling used in computer analysis.

[2]Sheehy, T. W., and Clark, D. R., A Method for Predicting Helicopter Hub Drag, Sikorsky Aircraft Division, United Technologies Corporation, USAAMRDL-TR-75-48, Eustis Directorate, U.S. Army Air Mobility Research and Development Laboratory, Fort Eustis, Virginia, January 1976, AD A021201.

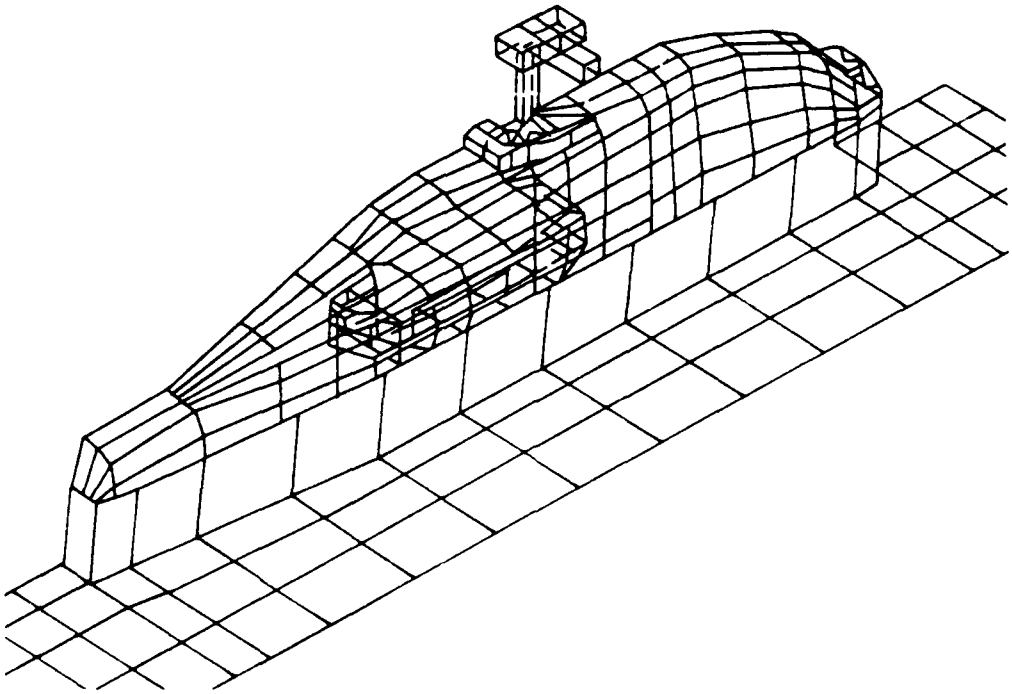

Figure 11. HPER paneling used in computer analysis.

NASA LANGLEY 4- BY 7-METER WIND TUNNEL TESTS

Procedure

The 0.8-scale model of the upper portion of the AH-64 was mounted onto the modified Navy HPER and tested in the 4- by 7-meter tunnel. This model was equipped with internal fans simulating airflow through the engine, transmission cooling radiators, engine compartment, and exhaust dilution system, as was the smaller scale model. These engine-simulator fans were immensely heavy, and mounting them so that their thrust could be measured directly would have caused difficulties in instrumentation. Since their mass flow rate and thrust were readily measured by dynamic pressure rakes in the ducts downstream of the fans, it was thought best to isolate the fans from the delicate forces and moments in other parts of the model. Thus, they were supported by the lower, nonmetric portion of the model and were ducted to the nacelle through short flexible ducting, which arrangement ultimately caused serious problems.

The HPER model was tested in the 4- by 7-meter tunnel at the dynamic pressures and velocities shown in Table 1.

TABLE 1. DYNAMIC CONDITIONS OBTAINED IN THE 4- BY 7-METER TUNNEL

Dynamic Pressure (lb/sq ft)	Velocity (kt)
69.0	240.9
47.8	200.5
27.2	151.2
12.5	60.7

Results

During these tests, the large model exhibited spurious pressure behavior and trends which suggested that blockage effects were more serious than anticipated. The test results include those that apply to the prototype vehicle configuration and those that apply to the complexities of the model systems.

As background to the discussion of wind tunnel modeling effects, the drag of the major airframe components is summarized in Table 2. This data indicates that the GRMS and HPER scale models developed similar drag levels for the hub and the pylon. In addition, the total vehicle drag measured by the GRMS agreed well with drag measured by the contractor's one-seventh scale model tested in a pressurized wind tunnel.

TABLE 2. DRAG BUILDUP BY COMPONENT

	Drag, D/q, sq ft	
Component	GRMS	HPER
Basic Hub	5.42	5.44
Pylon	4.97	5.26
Wing + Rockets	5.46	
Fuselage	7.45	
Empennage	2.50	
Total Vehicle		
No Wing/Rockets	20.34	
W/Wing + Rockets	23.40	
Controls + Mast	1.40	

Effects of Hub and Airframe Modifications. Evaluation of the hub and airframe modifications indicated strong scale effects as well as a sensitivity to engine airflow. The results of the testing indicated that, due to the hub and pylon interaction, the impact of a rotor head fairing must be evaluated in a flow environment as similar to actual conditions as possible. The effect of the hub fairing is shown in Figure 12 for the HPER model at a tunnel speed of 145 knots, hub rotation of 289 rpm, engine exhaust flow simulation, and baseline fuselage configuration. The hub fairing was tested with the covers both sealed and unsealed to the pitch arm at the inboard and outboard ends. The data show that the sealed, faired hub reduced total pylon and hub parasite drag by 0.8 square foot, while the unsealed, faired hub was relatively ineffective in reducing drag.

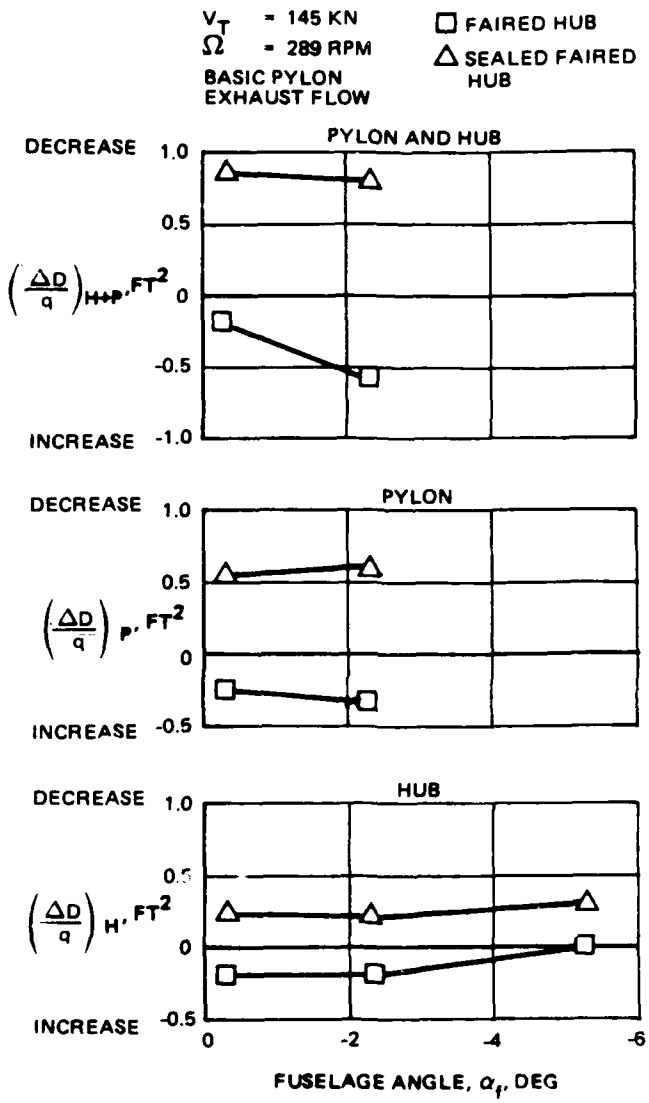

Figure 12. HPER hub and pylon drag reduction due to hub fairing.

The isolation of the pylon and hub components of parasite drag indicates that, for the HPER, most of the benefit of the sealed, faired hub came from the reduction in pylon parasite drag and not the reduction in hub parasite drag. This occurred even though there was no discernible change in the surface flow patterns on the pylon area of each configuration. The tufts applied to the pylon surface indicated no change in the separation regions behind the mast collar or the engine nacelle/pylon juncture. The surface pressure distributions also showed little difference. Similar results were shown for the nonrotationg hub case.

In the GRMS testing, similar drag reductions were demonstrated, but the distribution between hub and pylon was reversed insofar as effectiveness in drag reduction was concerned. As shown in Figure 13, the sealed, faired hub reduced the total pylon and hub drag by approximately 0.8 square foot, as measured during the HPER test. However, the majority of the drag reduction came from the hub. The drag reduction benefits of the sealed, faired hub in the GRMS scale were also shown by wake surveys at the tail empennage station.

The GRMS data also showed that sealing the faired hub made no difference in the drag reductions. The lack of change with sealing may be due to model size effect in that the cracks and gaps in the fairings became smaller faster than the overall scale reduction, generating a sealing effect.

The redistribution of the drag reduction components in the small-scale model and the difference in sealing effects indicate that the hub/pylon interaction is very sensitive and that rotor head fairing development work should be carried out on a scale comparable to the full-size hardware.

Another interesting result from the GRMS testing is that the removal of the beanie decreases hub drag even further due to reduction of hub cross section. However, drag reduction is not the complete story; flight testing of a similar beanie on the AH-64 indicated a marked reduction in tail vibration due to a reduction in turbulence.

In addition to these hub fairing modifications, several airframe modifications were evaluated in the tunnel: a modified nose gearbox fairing, a rotation of the stationary torque link, a modified doghouse, and boundary layer fences.

The nose gearbox fairing modification consisted of eliminating the bluff forward face formed by the engine nacelle and the nose gearbox. A fairing was wrapped around the nose gearbox and blended into the top and bottom of the engine nacelle in order to eliminate the area of flow stagnation formed by the forward nacelle face.

The rotation of the stationary torque link involved aligning the torque link parallel to a buttline and even with the mast, as opposed to the basic configuration of approximately 45 degrees to a buttline at aproximately 300 degrees azimuth.

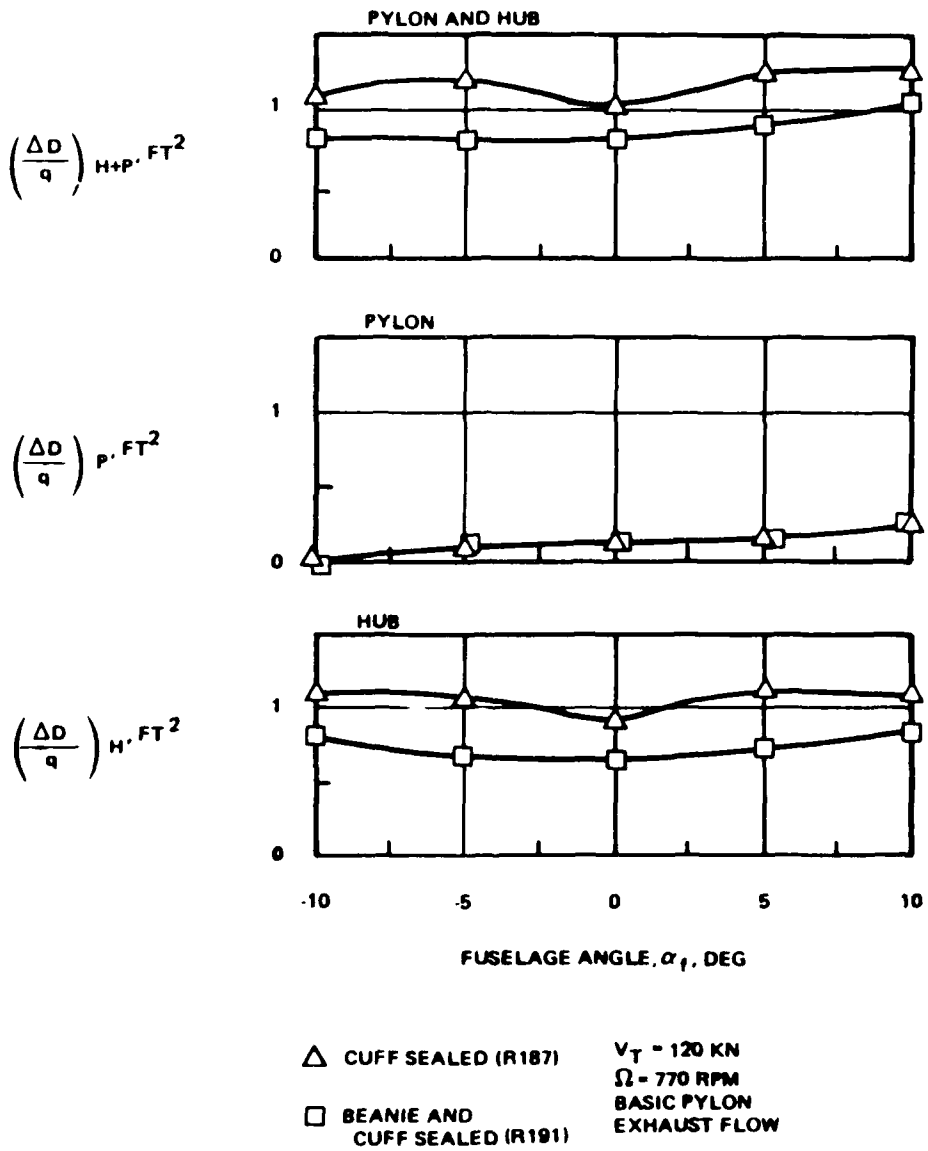

Figure 13. GRMS hub and pylon drag reduction due to hub fairing.

The drag impact of the airframe modifications is shown in Table 3 for both the GRMS and the HPER model testing. The comparison is presented at zero fuselage angle and the highest tested speed for each model: 145 knots for the HPER and 120 knots for the GRMS. The modified doghouse produces a small drag reduction in the GRMS but has no effect in the HPER, while the fences are less effective in the GRMS model than in the HPER model.

TABLE 3. DRAG INCREMENTS DUE TO AIRFRAME MODIFICATIONS

	Drag, D/q, sq ft		
Configuration	HPER	GRMS Basic hub	GRMS Rotor wake
Modified Doghouse	0	-0.15	-0.17
with Fences	0	-0.20	-0.26
Nose Gearbox Fairing	1.96	0.50	0.35
Torque Link Rotation	0.97		

It is felt that these differences are caused by the absence of engine airflow in the HPER testing. The AH-64 draws air from around the mast. During HPER testing the fans became inoperative, and testing continued without fan airflow and with the inlets sealed (the HPER drag reduction data are referenced to a baseline without airflow). The GRMS data were taken with full airflow simulation. The increased effectiveness of the torque link rotation indicates the sensitivity of the flow environment around the mast. Similarly, the reduced effectiveness of the boundary layer fences may indicate that the engine exhaust provides some boundary layer control over the aft pylon, reducing the separation the fences were intended to control.

Table 3 also shows the impact of the full main rotor wake. The GRMS data were recorded with the basic AH-64 hub for comparison with the HPER data, as well as with and without the GRMS rotor blades, to determine the effect of the rotor wake. The results of the comparison for the AH-64 model indicate that the inclusion of the main rotor wake supported the qualitative evaluation of the hub-alone data and produced a small increment of drag.

Pylon Drag. The effect of Reynolds number on pylon drag is shown in Figure 14. The data is presented as the ratio of pylon drag at a particular Reynolds number to the drag at a Reynolds number of 400,000. This ratio is then presented as a function of a scale unit Reynolds number defined using the tunnel speed and the model scale factor.

The data are presented as a ratio to eliminate certain engine airflow effects that will be discussed later. The condition considered is the basic AH-64 configuration at level attitude and with the basic hub rotating at the same hub tip speed (770 rpm for the GRMS and 289 for the HPER). A review of the data shown in Figure 14 indicates a critical Reynolds number of approximately 300,000; below this number, pylon parasite drag rises sharply.

It should be noted that the test conditions for the GRMS model in an atmospheric tunnel exceeded the critical Reynolds number only at the highest tested speed: 120 knots. This indicates that to record full-scale baseline drag data on a small-scale model, the tunnel should be pressurized to achieve a scale Reynolds number of 300,000. However, comparative data on different configurations under the same tunnel conditions may be acceptable without tunnel pressurization.

Simulated engine airflow effects on pylon parasite drag are shown in Figure 15. Corrected pylon parasite drag is presented as a function of mast inlet/mass flow ratio, which is defined as the square of the ratio of the flow into the mast inlet to the tunnel mass flow parameter formed by multiplying the tunnel density, tunnel speed, and exhaust area. Both GRMS and HPER pylon drag data are included for sealed engine/mast inlets, fan windmilling, inlet flow rate, and engine exhaust flow rate conditions. The HPER pylon drag data are corrected for tunnel blockage by increasing dynamic pressure by 14 percent, as discussed later.

The data are presented for the basic AH-64 configuration without a wing, with hub rotating, and at zero angle of attack. In addition, only data at scale unit Reynolds numbers greater than 200,000 are presented (a run number is presented at each data point for reference). The data include HPER runs from 60 to 145 knots and GRMS runs from 80 to 120 knots.

The pylon drag data indicate that there is a strong effect of inlet mass flow, particularly at low mass flows. Generally, the pylon drag is approximately 5.25 square feet, but below a mast inlet flow ratio of 0.04 the pylon drag rises sharply to a value of 9.3 square feet for sealed HPER conditions. For typical AH-64 mast inflow conditions at 145 knots, the pylon parasite drag is 6.6 square feet.

Several parameters were used in an attempt to correlate the HPER/GRMS pylon drag data, and only the mast inlet/mass flow ratio was used successfully. The data showed a great deal of scatter when total mass flow or nacelle mass flow was used, probably due to the manner in which mass flow level was varied. To simulate exhaust mass flow levels, the fans drawing air in both the engine nacelle inlet and the mast inlet were set at maximum settings. To simulate inlet mass flow levels, the reduction in fan setting was greater for the fans drawing air from around the mast than for the fans drawing air from around the nacelle inlet. Consequently, the flow changes were greatest through the mast inlet, and this flow parameter proved dominant. This indicates that when powered models are tested, extreme care should be taken to accurately simulate the full-scale vehicle airflow environment.

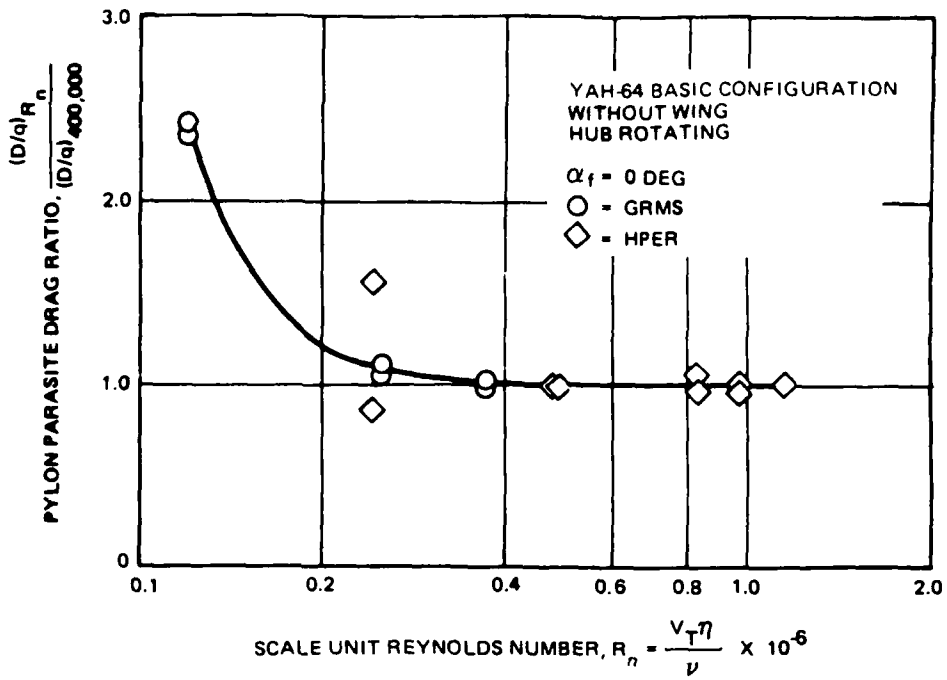

Figure 14. Effect of Reynolds number on pylon parasite drag.

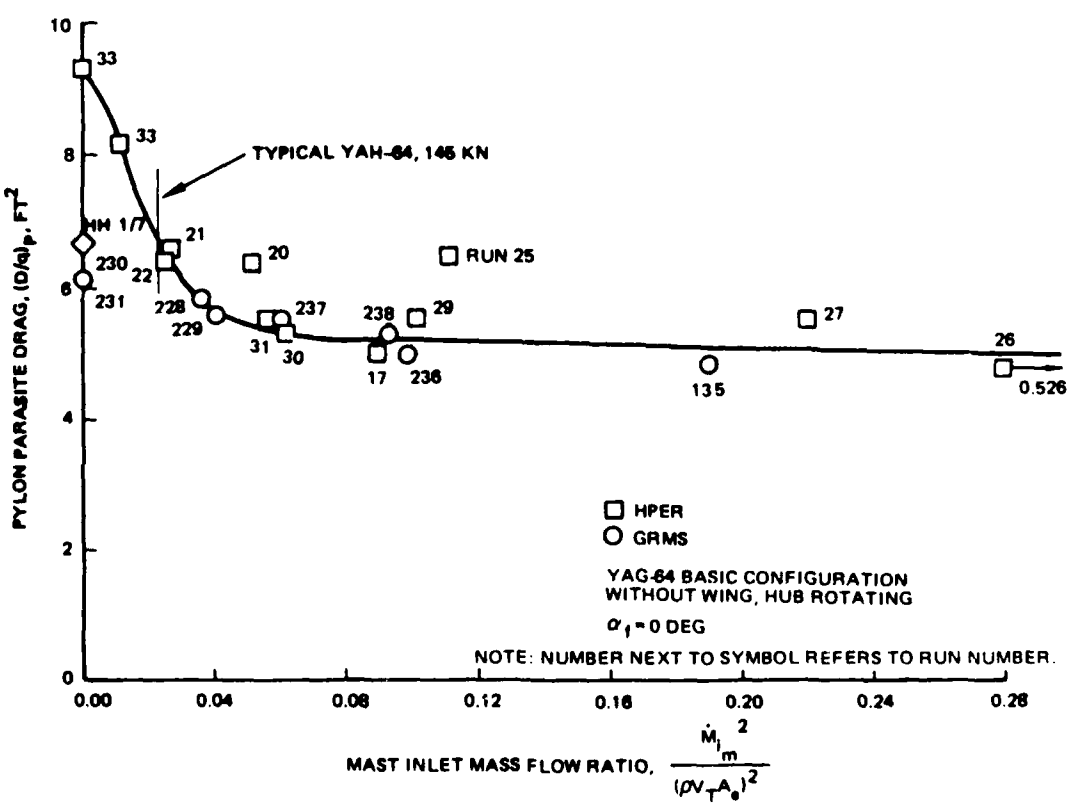

Figure 15. Effect of mast inlet mass flow on pylon parasite drag.

Differences in model sealing are evident at zero mast inlet/mass flow ratios. The sealed HPER model shows substantially higher pylon drag than the sealed GRMS model due to the method of sealing the mast inlet. In sealing the HPER model mast inlet, only the fan inlets were sealed, leaving the cavity open around the mast. In sealing the GRMS model mast inlet, however, the mast cavity was sealed over to form a smooth contour, which resulted in lower drag. It is interesting to note that the pylon parasite drag is estimated to be 6.7 square feet based on Hughes Helicopters data taken on a one-seventh scale solid model without engine flow, at a scale unit Reynolds number of 350,000.

Effects of Model Scale and Engine Mass Flow. The effect of model scale or Reynolds number can be isolated because identical aircraft components were tested at two different scales in the same tunnel under identical conditions. The effect of Reynolds number on hub drag is shown in Figure 16 for both the basic hub and the sealed, faired hub. Both the GRMS and the HPER hub data are presented at the same hub tip speed. The Reynolds number in this case is based on the tunnel speed and model scale factor. It can be seen that the hub data correlate well with a sharp rise in hub drag beginning between a Reynolds number of 250,000 and 300,000. The same Reynolds number behavior is shown for the sealed, faired hub. The drag reduction due to sealing the fairing is consistent over the whole Reynolds number range, except at the highest speed, where the drag reduction diminishes due to an increase in sealed, faired hub drag relative to the basic hub. The GRMS and HPER hub models were fabricated in an identical manner, with the edges of the various hub components (such as the lead-lag dampers) rounded to match the actual components. Since the geometries are virtually identical, the drag rise associated with Reynolds number is attributed to the transition from super- to subcritical Reynolds number and the corresponding rise in drag.

The effect of Reynolds number can also be seen in the fuselage drag. Figure 17 presents the variation in GRMS fuselage drag both with Reynolds number and with engine mass flow levels. In this case the fuselage measures all body forces except the tail empennage, rotor hub, engine nacelles, or other parts of the pylon. The critical Reynolds number of 250,000 is again evident. In the case of the fuselage, however, this drag decreases as Reynolds number decreases. This may be due to the engine mass flow creating a unique flow field that interacts with the tunnel flow at low tunnel speeds. As can be seen, the engine mass flow does have a pronounced effect that depends on configuration.

Above the critical Reynolds number, engine mass flow levels do not affect the fuselage drag for configurations without the wing. With the wing, however, the level of mass flow produces an incremental drag due to the interaction of engine airflow and wing. In this case, the model internal pressure was measured and any model pressure differential induced by the fans was removed. This demonstrates again that the total helicopter configuration should be modeled to measure drag accurately.

Hub Drag. An analysis of the large- and small-scale data indicates that hub rotation had a distinct effect on hub drag and that the effect was modified by both scale and fuselage angle of attack.

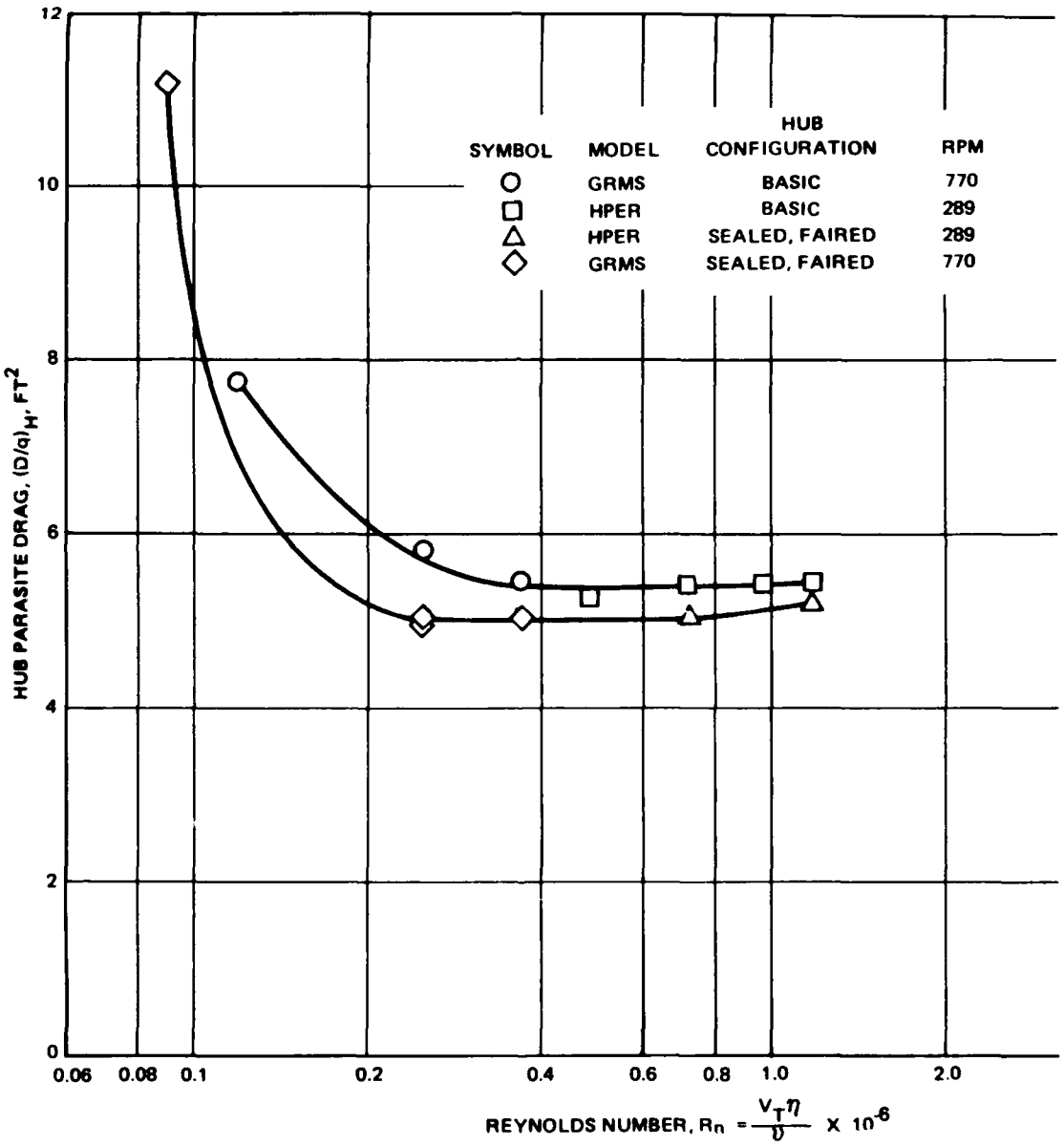

Figure 16. Effect of Reynolds number on hub drag.

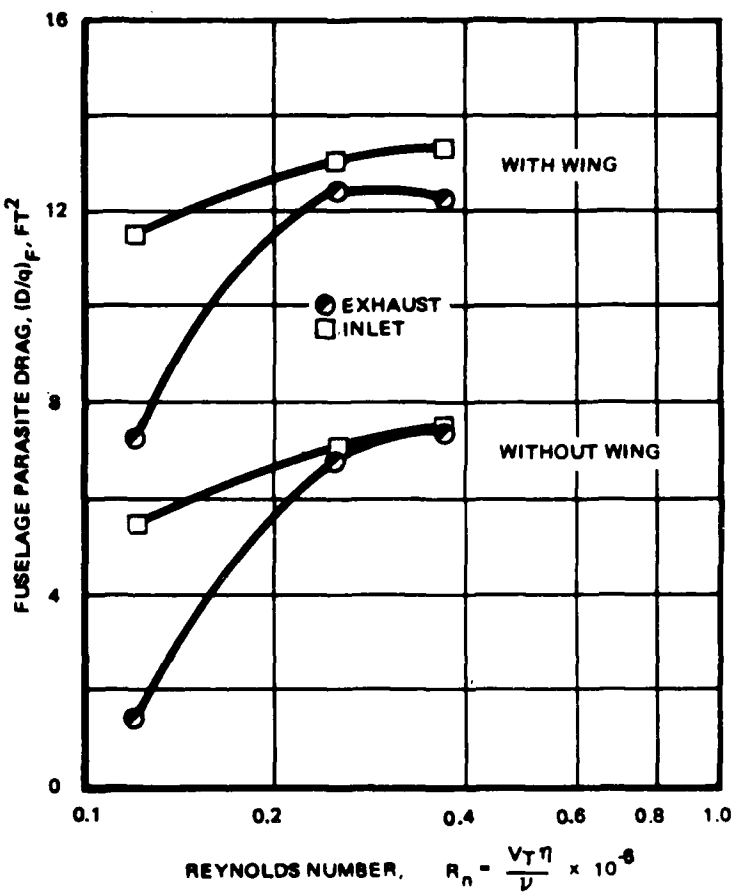

Figure 17. Effect of Reynolds number on fuselage drag (GRMS).

The effect of hub rotation on the large-scale data is shown in Figure 18 for the basic hub and for the sealed, faired hub. The data are presented at 60 knots, but due to data recording problems, only one fuselage angle is shown for each hub configuration. For both hub configurations, the rotation of the hub resulted in a 0.5-square-foot increase in hub parasite drag at 60 knots. This drag increment was fairly consistent over the complete tunnel speed; the drag increment due to rotation increased linearly with rotational speed. For the sealed, faired hub, the drag increment was linear in two stages with a transition at the mid-RPM range, indicating a transition phenomenon.

The hub drag data were also examined on the basis of the hub advance ratio (the ratio of tunnel speed to hub rotation speed), but the analysis produced no clear trend.

A trend similar to the HPER data for increased drag with the hub rotation is shown in Figure 19 for the GRMS data. For the GRMS hubs, however, angle of attack modifies the effect. For both the basic and the sealed, faired hubs, an approximately 0.5-square-foot increase in hub drag is shown at 10 degrees of fuselage angle of attack. However, at zero angle of attack, hub rotation above 100 rpm had little effect on hub drag. This was seen in the HPER data and may be a Reynolds number effect.

For both the GRMS and the HPER data, the pylon drag was unchanged by hub rotation. This may be due to the unique configuration of the AH-64 rotor and mast, in which the hub is supported by a stationary mast and driven by a shaft inside the stationary mast. On most other helicopters, the hub is supported and driven by the same mast. Consequently, the disturbance created by rotation is close to the pylon. The AH-64 configuration confines rotation to the immediate hub area. This indicates that hub rotation may not be required for pylon drag studies on stationary mast helicopter configurations.

Summary of Findings

1. Engine inlet and exhaust flow is significant for helicopter drag studies.

2. Drag reduction of typical helicopter components is an aggregate of small beneficial flow changes, with no one change being dramatic.

3. Hub fairings must be sealed to affect drag to any significant degree.

4. Hub rotation increasesd hub parasite drag by approximately ½ square foot.

5. Hub and pylon parasite drag can be reduced about 1 square foot from the unmodified values by careful and extensive fairing and sealing techniques.

6. Drag reduction studies without full main rotor wake can provide significant knowledge provided the speed range is appropriate.

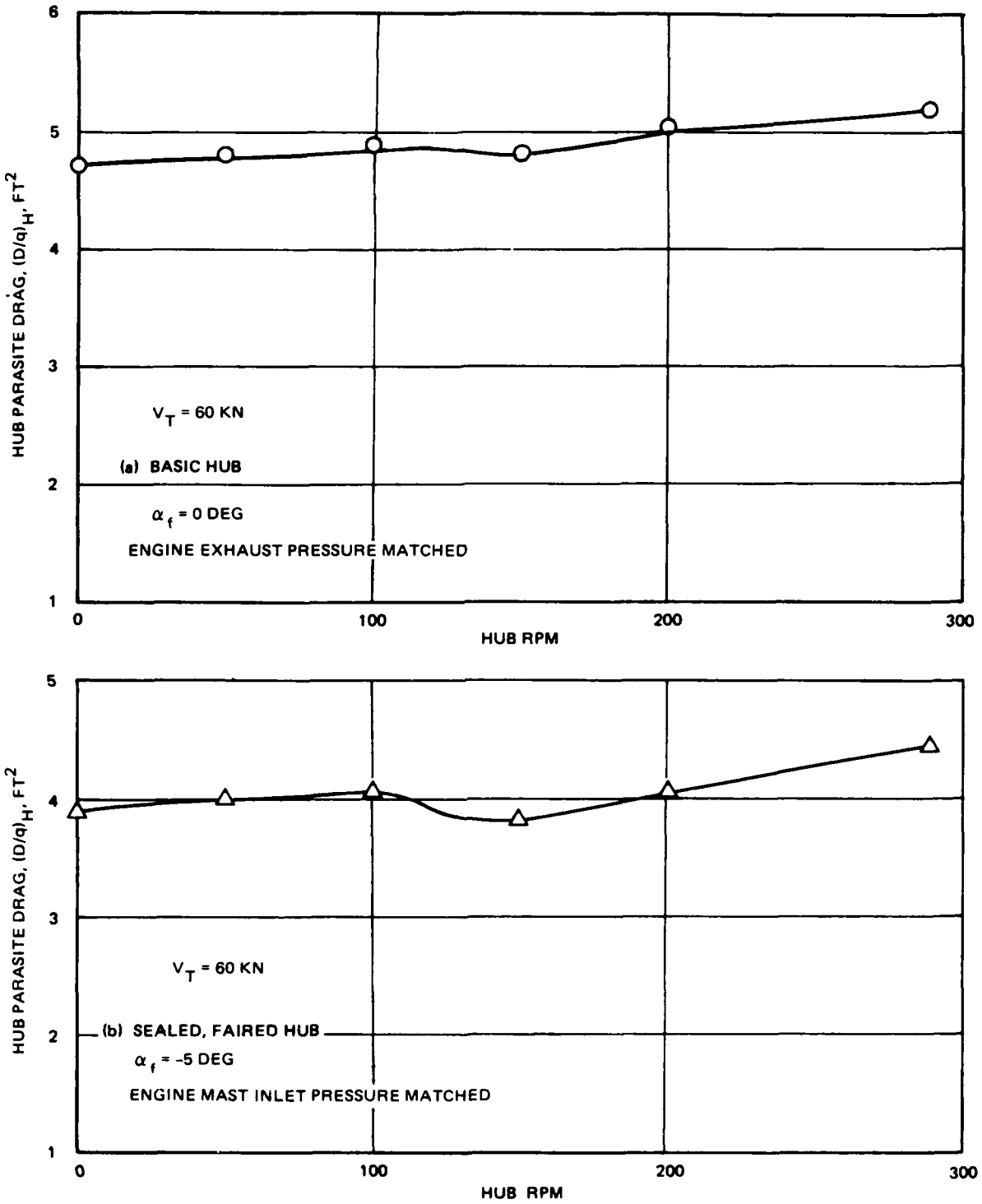

Figure 18. Effect of hub rotation on HPER hub drag.

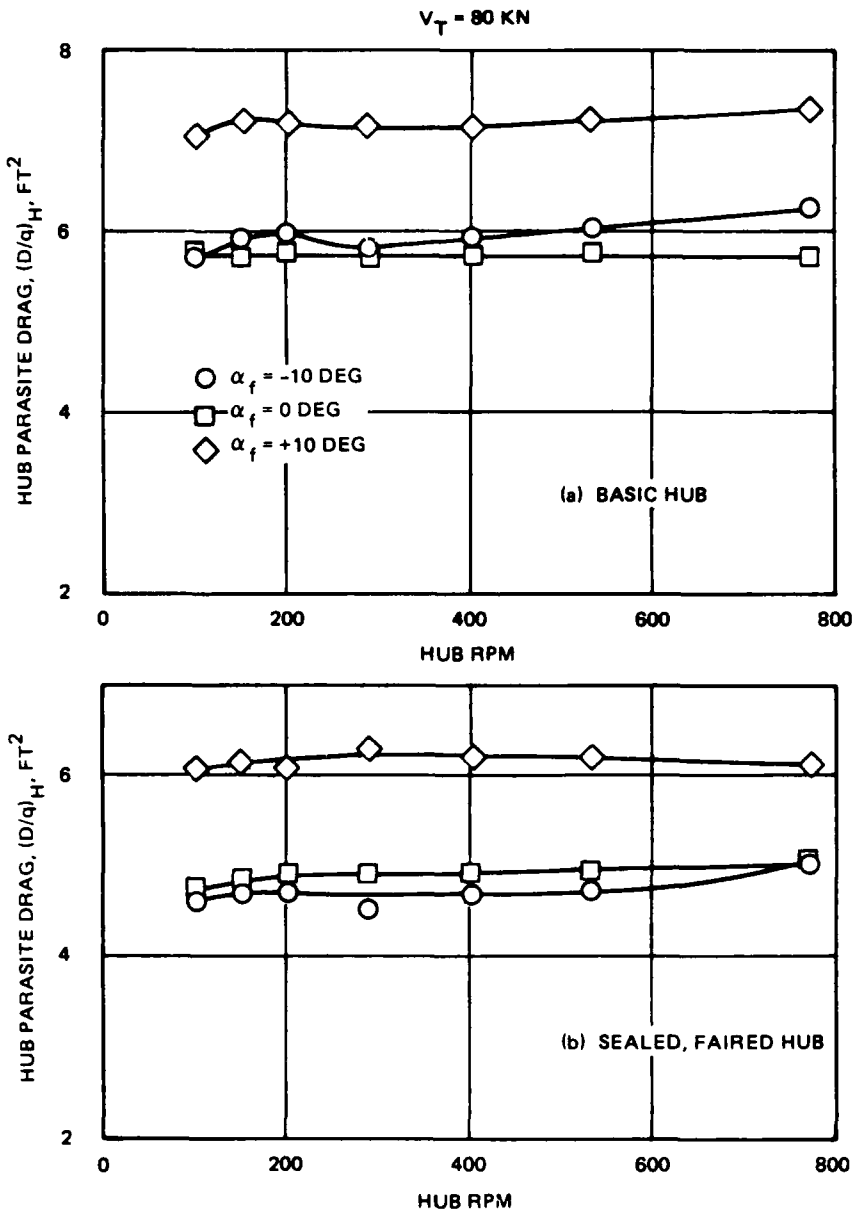

Figure 19. Effect of hub rotation on GRMS hub drag.

7. Pylon drag is unchanged by hub rotation.

8. A Reynolds number of at least 300,000 is needed to simulate full-scale airflow behavior on the AH-64.

9. Main rotor mast inflow has a noticeable effect on pylon drag.

10. The AH-64 Apache wing has a favorable effect on engine nacelle drag.

11. Flow over the aft pylon is very sensitive to angle of attack.

12. Downwash angles at the stabilator did not exceed 47 degrees.

13. There is considerable asymmetry in the main rotor wake.

14. There is a predominant sidewash to the right, apparently due to the effect induced by the rotor hub.

15. Strakes down the back of the pylon had a minor effect on wake behavior in the wind tunnel (they were beneficial enough on the actual vehicle to be incorporated in subsequent production).

Additional findings included the following three problems to be resolved before or during further testing:

1. The flexible ducting used in the engine-simulation fan mounting caused erroneous thrust readings and prevented clear delineation of inlet lip suction, internal duct drag, and exhaust thrust. (It had been known that a spiral-reinforced flexible duct develops longitudinal force when it is pressurized, but in these tests, the longitudinal force changed to a much more disturbing degree than anticipated.)

2. Due to the structural arrangement of the modified HPER, the new main balance had to be installed at the front end of that part of the model whose forces and moments were to be measured. This extreme position of the balance made the entire portion suspended from the balance tail heavy even under static load. When dynamic loads were imposed, this suspended part of the model often touched or "grounded" against the fixed, nonbalanced portion of the model, rendering invalid any force measurements under these conditions.

3. Blockage effects were more serious than anticipated because a model of the dimensions of the HPER was too large for the NASA Langley 4- by 7-meter tunnel.

CORRECTIVE MEASURES PRIOR TO FULL-SCALE TUNNEL TESTS

During the time period between the 4- by 7-meter tunnel tests and the full-scale tunnel tests, the HPER and its model shell were modified as follows to correct problems uncovered during the 4- by 7-meter tunnel tests:

1. The problem with flexible ducting was corrected by hard-mounting the engine simulation fans to the nacelle itself (they had been hard-mounted to the foundation of the model and ducted to the nacelle via flexible ducting), so that the thrust of the entire nacelle assembly would be measured as a unit.

2. The tail heavy condition of the metric portion of the model was corrected by adding an instrumented link at the problem point.

The original AH-64 Apache mast inlet configuration was a "horse-collar" shape, which acted as an air-dam in urging the local airflow into the inlets for cooling air for the transmission coolers, and subsequent use as engine nacelle cooling. In the time between tests in the 4- by 7-meter tunnel and the full-scale tunnel, the manufacturer developed an improved mast inlet for increasing airflow rates into the internal cooling system and improving the steadiness of this flow. This inlet had been fitted to one flight test aircraft and had shown some promise of flow improvement. This configuration was fabricated and tested on this model (and was subsequently incorporated in the production vehicles).

The Safety and Survivability Technical Area of AATD developed an exhaust system designed to suppress the exhaust infrared signature. Even though the model provided only cold flow, the external shape of this configuration was tested to determine its effect on overall aerodynamic drag. The change in aerodynamic drag over the prototype exhaust configuration proved to be less than the instrumentation noise.

HPER TESTS IN FULL-SCALE WIND TUNNEL

Figure 20 shows the HPER in place in the 30-foot-high by 60-foot-wide test section of the full-scale tunnel in 1982. The model is placed on the groundboard, which is elevated 15 feet above the floor level of the open test chamber. The new mast inlet has been installed on the model, and the old mast inlet is shown on the test section floor in the foreground. The model was installed during maintenance and repair of the drive motors, shown in Figure 21.

It was hoped that there would be sufficient overlap in the operating conditions of the two tunnels to permit comparison of pressure data from both tunnels at the same operating conditions, but the two tunnels had operational limitations which together prevented this. The 4- by 7-meter tunnel exhibited flow instabilities in the test section at velocities below about 60 knots, and main drive motor mount vibrations in the full-scale tunnel prevented obtaining any velocities greater than 60.7 knots.

Table 1 listed the dynamic conditions obtained in the 4- by 7-meter tunnel tests, and Table 4 lists the dynamic pressures and velocities obtained in the full-scale tunnel tests. A comparison of Table 4 with Table 1 shows that there was only one velocity obtained in both tunnels - 60.7 knots - which severely limited the comparison of data.

TABLE 4. DYNAMIC CONDITIONS OBTAINED IN THE FULL-SCALE TUNNEL

Dynamic Pressure (lb/sq ft)	Velocity (kt)
03.2	30.7
04.7	37.2
07.6	47.3
12.5	60.7

MATRIX OF TEST VARIABLES

Table 5 lists the model variables and their ranges. Variable changes were performed in decreasing order of complexity or time consumption, with model pitch change being performed least frequently (it took 6 minutes from limit to limit), then tunnel rpm (and therefore dynamic pressure), then engine

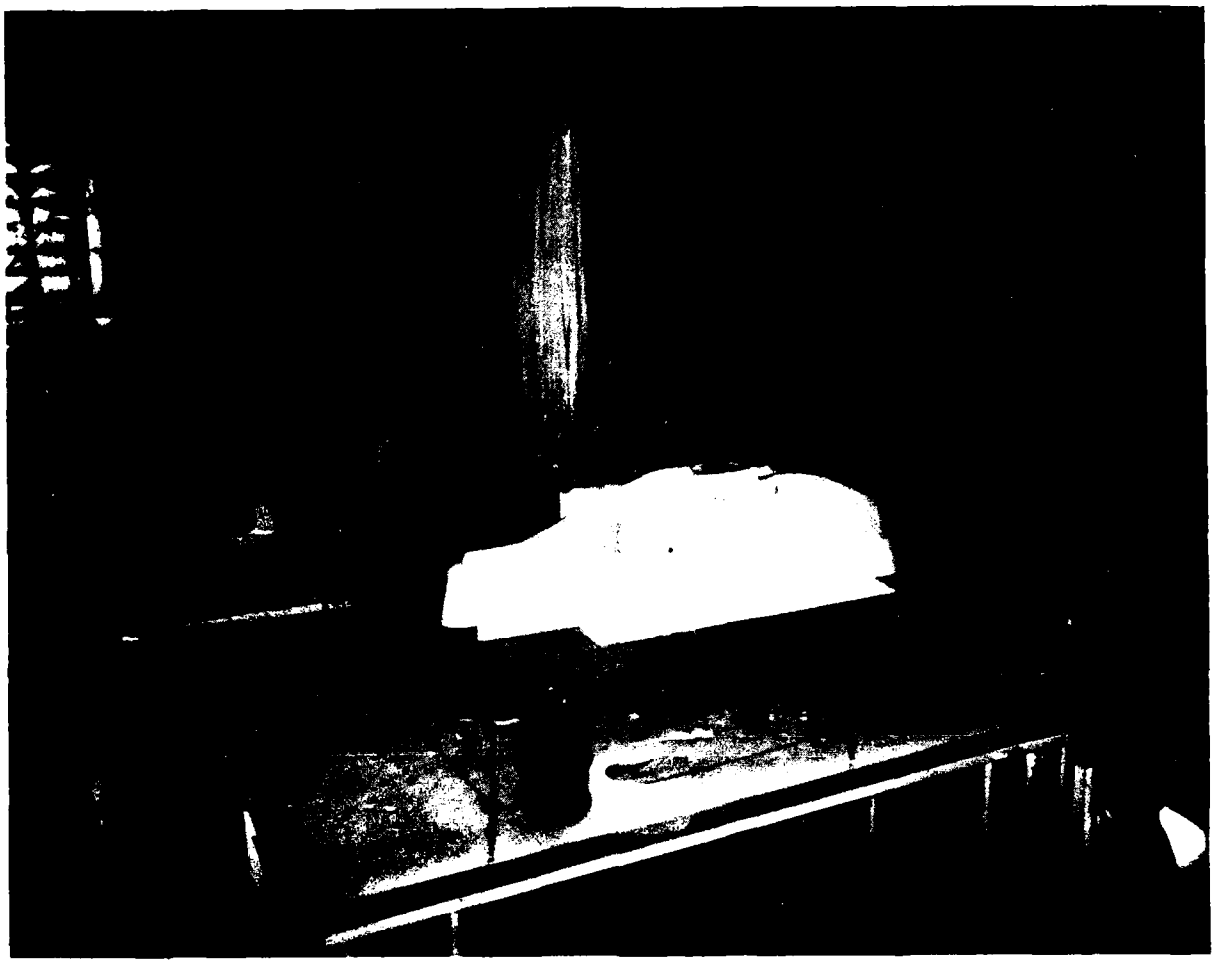

Figure 20. HPER model in full-scale tunnel.

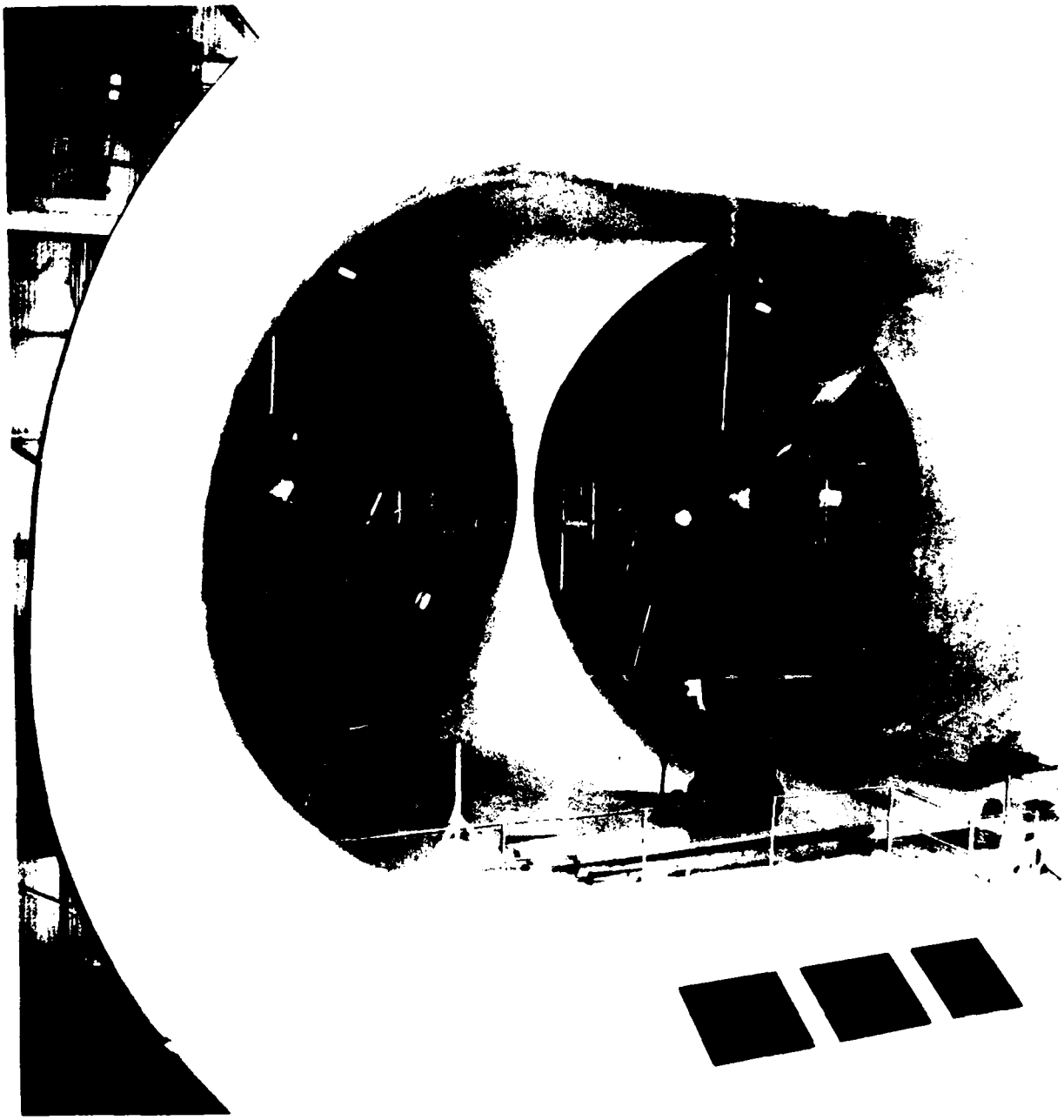

Figure 21. Full-scale tunnel drive unit servicing.

simulator fan speed, with hub rotation ON or OFF as the simplest configuration change, and therefore performed most often. This arrangement resulted in a typical matrix of test data points as shown in Table 6. The baseline configuration was tested first to ensure the measurement of the most important parameters before repeated operation of the complex model operational and instrumentation systems started causing breakdowns. The improved mast inlet was then installed and tested, followed by runs with the alternate exhaust exit ducts, with strakes and with tufts.

TABLE 5. VARIABLES IN FULL-SCALE TUNNEL TESTS

VARIABLE	RANGE
Tunnel Dynamic Pressure	0 to 12.5 psf
Tunnel Velocities	0 to 60.7 kt
Fan Drive Pressure	0 to 94 psi
Model Pitch Angle	0 to -7 deg
Hub Rotation	On or Off

GENERAL INSTRUMENTATION PROBLEMS

Gathering meaningful data from small differences in large numbers is a hazard in any instrumentation system, and in these tests it was aggravated by two separate situations:

1. Because the main balance had to be large enough to support the entire metric portion of the model, its measurement capacity in all directions was large.

2. Because of drive system problems in the full-scale tunnel, maximum dynamic pressure was 12.5 pounds per square foot, equivalent to only 60.7 knots.

To further compound the instrumentation problems, in the 4- by 7-meter tunnel tests the large static preload permitted the aft portion of the pylon to touch the nonmetric portion of the model under some dynamic loading conditions. When this occurred, measurements in any direction were invalid. To correct this condition for the full-scale tunnel tests, an instrumented link was installed at the aft end of the pylon to take some of the load, so that the main balance was not so drastically preloaded.

TABLE 6. TYPICAL MATRIX OF TEST DATA POINTS

Point Nr.	Run Nr.	Pitch Angle	Dynamic Pressure	Fan Power	Hub Rotation
1	1	0	12.04	Zero	On
2	2	0	12.04	Zero	Off
3	3	0	12.04	Low	On
4	4	0	12.04	Low	Off
5	5	0	12.04	High	On
6	6	0	12.04	High	Off
7	7	0	07.50	Zero	On
8	8	0	07.50	Zero	Off
9	9	0	07.50	Low	On
10	10	0	07.50	Low	Off
11	11	0	07.50	High	On
12	12	0	07.50	High	Off
13	13	0	04.69	Zero	On
14	14	0	04.69	Zero	Off
15	15	0	04.69	Low	On
16	16	0	04.69	Low	Off
17	17	0	04.69	High	On
18	18	0	04.69	High	Off
19	19	0	03.31	Zero	On
20	20	0	03.31	Zero	Off
21	21	0	03.31	Low	On
22	22	0	03.31	Low	Off
23	23	0	03.31	High	On
24	24	0	03.31	High	Off
25	25	-4	12.04	Zero	On
26	26	-4	12.04	Zero	Off
27	27	-4	12.04	Low	On
28	28	-4	12.04	Low	Off
29	29	-4	12.04	High	On
30	30	-4	12.04	High	Off
31	31	-7	12.04	Zero	On
32	32	-7	12.04	Zero	Off
33	33	-7	12.04	Low	On
34	34	-7	12.04	Low	Off
35	35	-7	12.04	High	On
36	36	-7	12.04	High	Off

Etc.

ANALYSIS OF RESULTS

One objective of these tests was to resolve the blockage problem that appeared in the tests in the closed-section 4- by 7-meter tunnel by testing the same model in the full-scale tunnel and comparing the data. For this to provide valid data, the two tunnels had to provide adequate overlap of operating conditions. This was not the case. Maximum velocity in the full-scale tunnel just matched the minimum velocity in the 4- by 7-meter tunnel. Therefore, only a small portion of the data from the two tunnels was available for comparison, as originally intended.

Another objective of the tests was to examine the effectiveness of corrections applied to the test device itself, following the earlier tests in the 4- by 7-meter tunnel, as a separate issue from the aerodynamic considerations. In the earlier tests, certain defects in the test device had emerged to a troublesome degree. In order to improve wind tunnel test device techniques, and to determine what effect these defects might have had on the data from the earlier tests, considerable effort was expended on this objective.

Other issues addressed in the tests are discussed in the following paragraphs. Some of these issues are related to one another, but a few are individual, fragmented problems worked on for the sake of their own resolution.

Blockage

Analytical comparison of data from the 4- by 7-meter tunnel tests was reported in Reference 1. Selected plots from this document are presented here for comparison to the results from the tests in the full-scale tunnel. In the 4- by 7-meter tunnel, the differences between the pressures measured on the fuselage of the 0.3-scale model and the 0.8-scale model were greater than expected.

Since the models agreed well with each other geometrically, auxiliary tests were performed to establish the possible source of these differences.

Pressure surveys of the tunnel ceiling were correlated with model surface pressure readings. Typical pressure data is shown in Figures 22 and 23. The results of this survey led to the conclusion that the differences in the data from the two scale models was due to blockage due to the size of the HPER model.

In the tests of the HPER in the 4- by 7-meter tunnel, the corrections required for dynamic blockage and for velocity blockage were both large, but of differing value. Further, they had different longitudinal variations, which was not expected. The blockages were both so large that the tunnel staff decided to group them into one value, as discussed in Reference 1. This mean value was applied to the appropriate 0.8 scale data, which brought it closely into line with the 0.3 scale data. This data is shown on Figures 24 and 25.

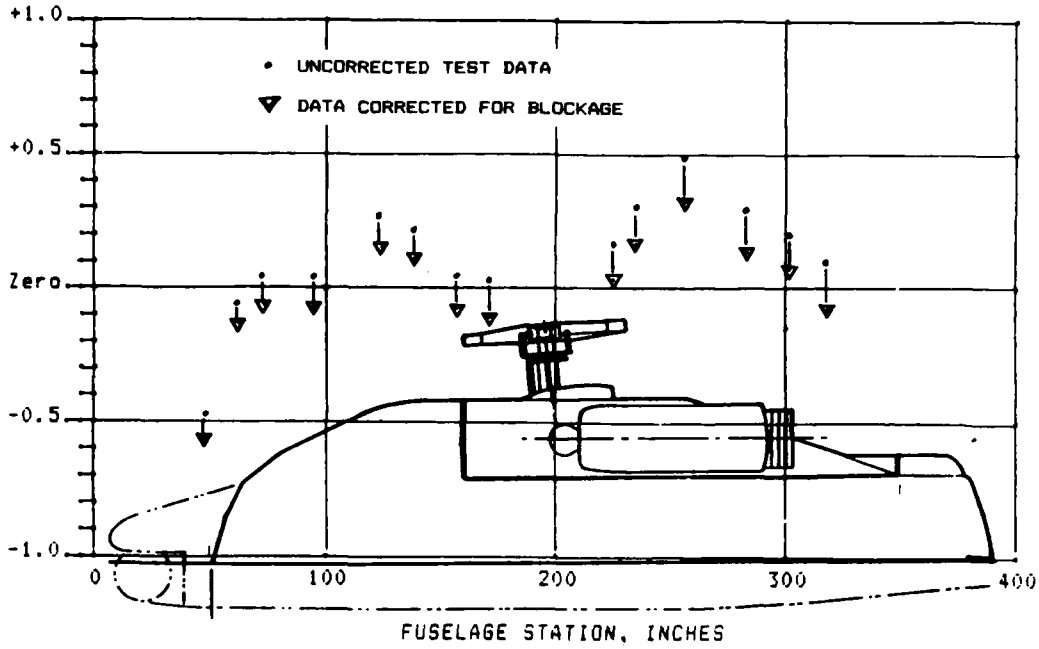

Figure 22. Blockage corrections applied to HPER data from NASA Langley 4- by 7-meter wind tunnel along Buttline 5.

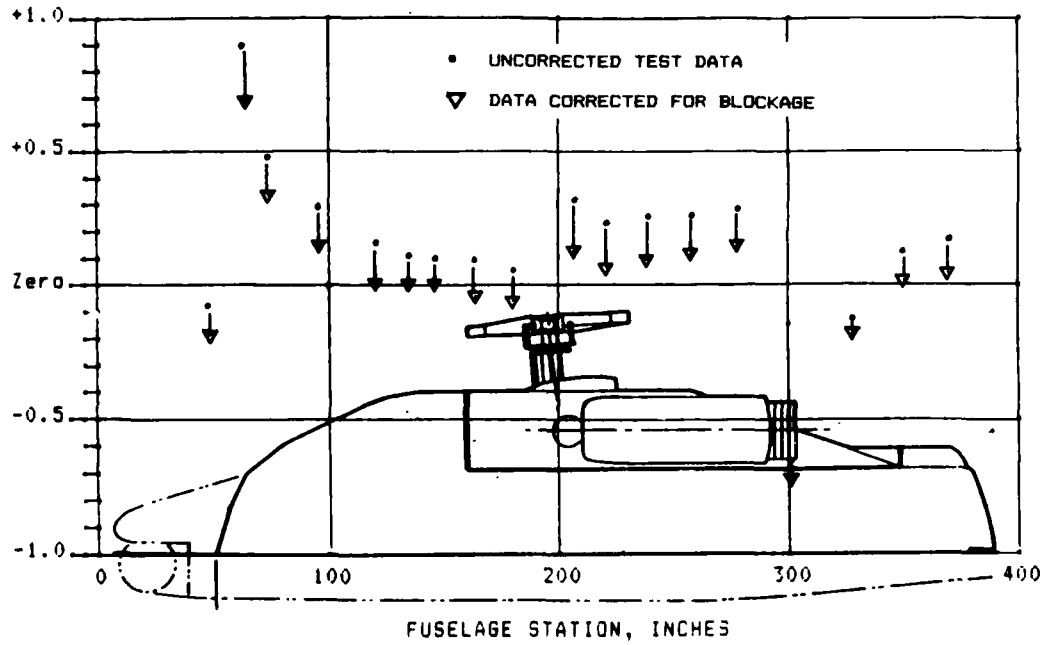

Figure 23. Blockage corrections applied to HPER data from NASA Langley 4- by 7-meter wind tunnel along Waterline 132.

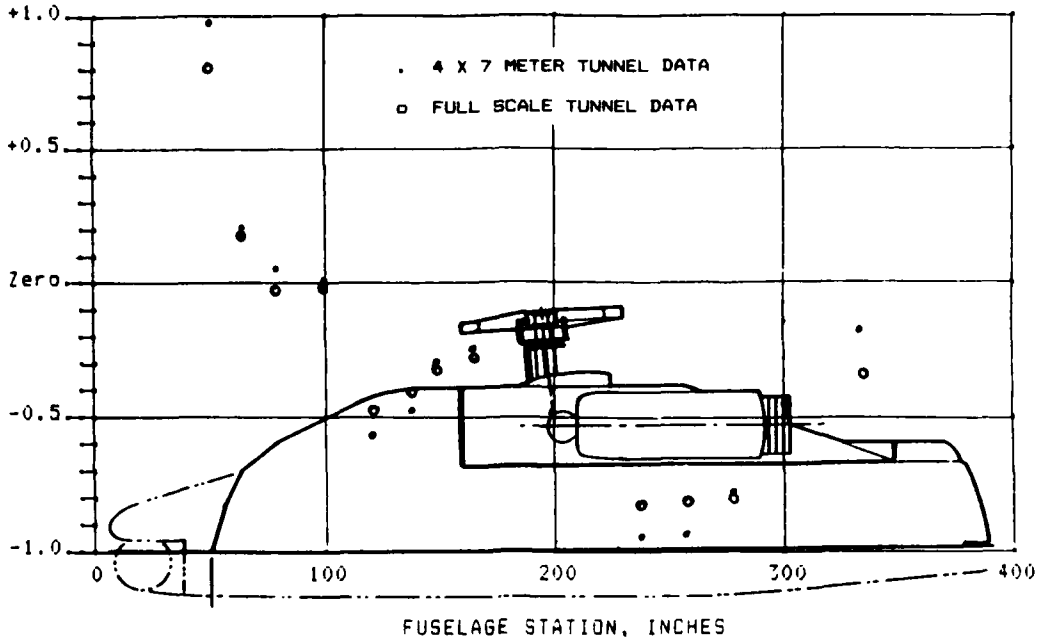

Figure 24. Fuselage surface pressure coefficient data from HPER tests in NASA Langley full-scale tunnel along Buttline 5 compared to similar data from tests in NASA Langley 4- by 7-meter tunnel.

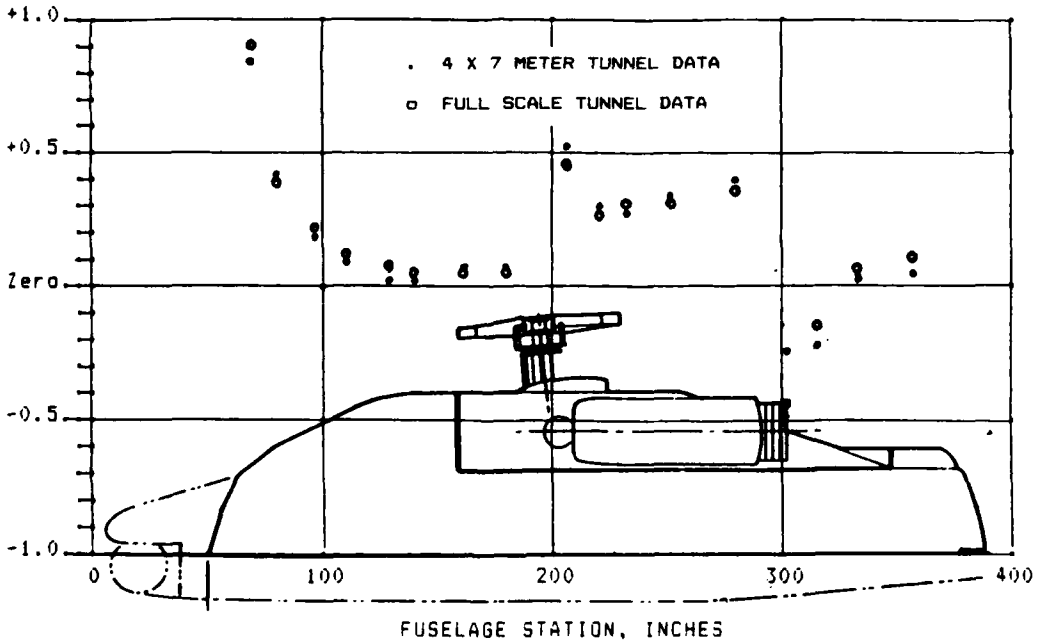

Figure 25. Fuselage surface pressure coefficient data from HPER tests in NASA Langley full-scale tunnel along Waterline 132 compared to similar data from tests in NASA Langley 4- by 7-meter tunnel.

Effects of New Mast Inlet Design

Longitudinal force measurements were taken with varied engine-simulator/fan power settings for the improved mast inlet design as compared with the old design. "High" fan power represented cruise power, "Zero" fan power provided a zero point on the data curves, and "Low" fan power provided an intermediary point for data plotting.

The new mast inlet may be evaluated from another aspect by a means plot of pylon longitudinal force (thrust to the left and drag to the right) versus tunnel dynamic pressure, with a separate curve for each fan power setting (see Figure 26). The solid curves represent data for the original inlet and the dashed curves represent the new mast inlet. The "fans high" and "fans low" pairs of lines of data indicate that the new inlet provided approximately 1/8 square foot drag decrease at the high tunnel dynamic pressure. The "fans zero" pair of lines of data show that the redesigned inlet caused almost no change in the drag.

This data indicates that drag reduction benefits of the new mast are insignificant and inconsistent. This implies that the new mast inlet configuration need not be installed on the prototype vehicle for drag improvement reasons. However, the improvement in the quality and smoothness of the airflow used for transmission and nacelle cooling may be significant enough for such an installation. (An interesting side point: with the fans set at cruise power, the residual thrust just cancels pylon drag at 52 knots.)

Strakes

The upper aft surface of the fuselage was fitted with aerodynamic strakes in an effort to smooth out the wake from that region, which impinges on the tail surfaces and tail rotor of the prototype. The tests in the 4- by 7-meter tunnel did not show a definitive improvement in airflow quality, but the manufacturer has incorporated strakes on the production vehicles.

Pylon Drag

At zero tunnel dynamic pressure, with the fans set at maximum power, the fan duct pressure rakes registered a total of 296 pounds of fan thrust. The pylon balance registered 135 pounds. The difference, 161 pounds, may be attributed to duct losses, 54.39 percent of fan thrust. At maximum tunnel dynamic pressure, with the fans at maximum power, the rakes measured 306 pounds of fan thrust and the pylon balance registered 40.7 pounds of thrust.

The increase in dynamic pressure provided sufficient inlet ram to place the fans in a more efficient operating environment, resulting in a 3.3 percent increase in fan thrust. On the assumption that the duct losses held steady at 54.39 percent, the calculated net fan thrust was 140 pounds. Pylon drag reduced this value to 40.7 pounds at the pylon balance, so the pylon drag must have been 99.3 pounds at this dynamic pressure. This compared well with the 94.7 pounds measured in the 4- by 7-meter tunnel tests.

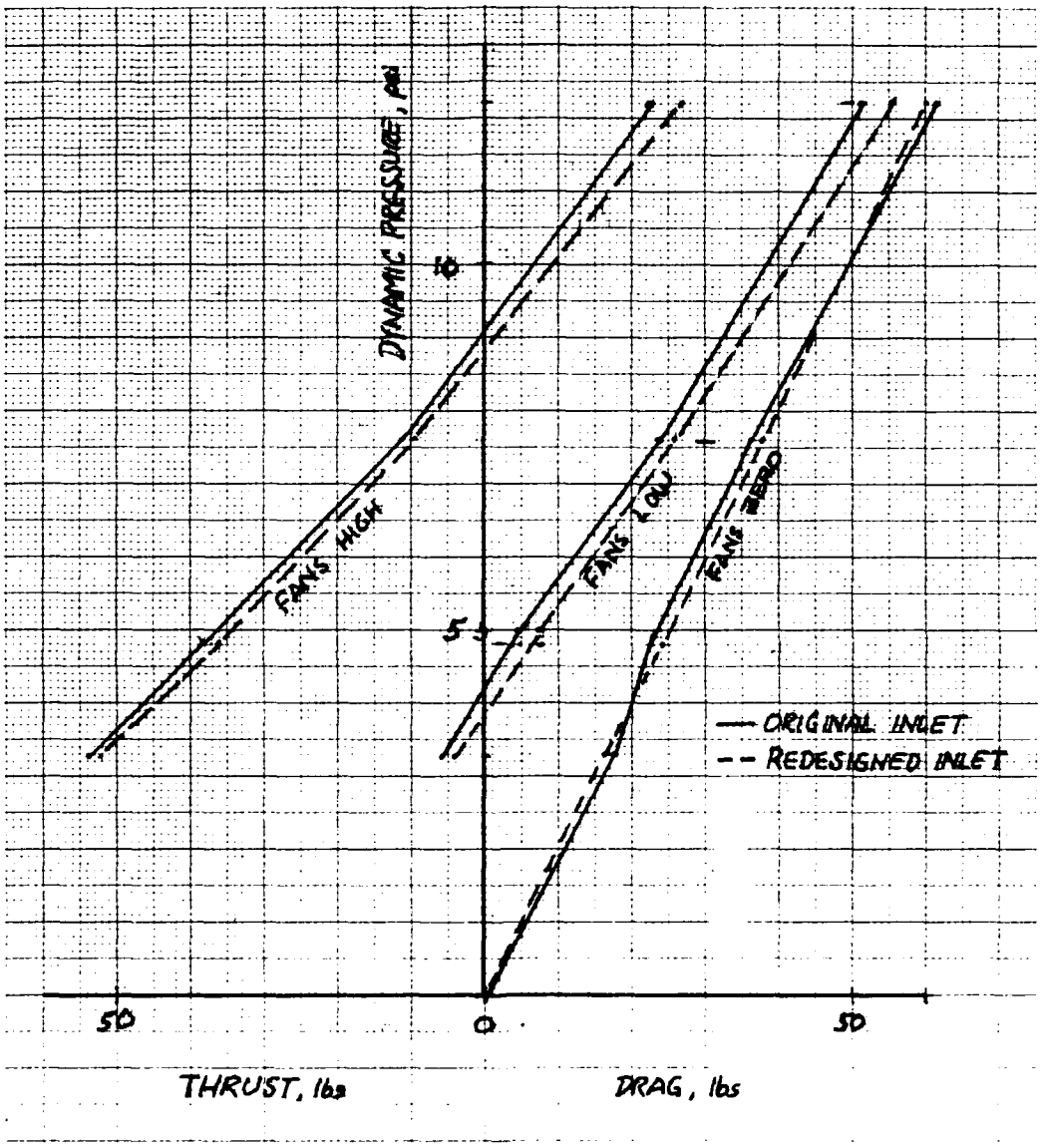

Figure 26. New mast inlet data.

This value of D = 99.3 pounds divided by the tunnel dynamic pressure of 12.04 pounds per square foot yields a D/q or equivalent flat plate drag of 8.3 square feet.

Effect of Fan Thrust on Pylon Pitching Moment

Several pitching moment readings were examined at conditions of fuselage level, 4 and 7 degrees nose down, at tunnel dynamic pressures from zero to maximum. Since the engine-simulation fans were mounted well above the pylon balance, variations in fan thrust should have resulted in appropriate variations in pylon pitching moment.

A redundant pitch link was necessary to prevent the instrumented portion of the model from touching the noninstrumented portion at the rear of the model, due to the tail-heavy condition of the instrumented portion. The link readings were in parallel with the main balance readings, which could have caused force and moment resolution difficulties. As shown in Table 7, the results were predictable, fairly smooth, and linear, substantiating that the redundant pitch link was designed and installed properly.

TABLE 7. EFFECT OF TUNNEL DYNAMIC PRESSURE ON FAN THRUST

Point	Tunnel RPM	Tunnel Q	Lt. Fan	Rt. Fan
1158	0	00.00	150.9	119.0
1150	100	03.31	147.0	121.4
1143	120	04.69	151.7	122.8
1136	150	07.50	147.3	120.7
1129	190	12.04	146.7	127.8

Note that the thrust of the left fan decreases slightly with dynamic pressure, while the thrust of the right fan increases. This variation might have been due to flow angularity, either inherent in the tunnel or caused by the presence of the model. The tunnel has a double-toroidal configuration, with each toroid providing the flow for half of the test section, which might account for some asymmetry down the centerline of the test section. The full-scale tunnel staff did not consider this asymmetry to be significant, for it was their choice to place the model on the centerline and very near the leading edge of the ground plane.

Other items which might have contributed to this asymmetry were differences in the internal ducting downstream of the fans, irregularities in the angular settings of the vanes internal to the infrared suppression exhaust outlets, or asymmetries in the model structure ahead of the fan inlets.

Duct Losses

The engine-simulation fans provide a more nearly correct inlet and exhaust environment for the rest of the model than would be provided by simple flow through open ducting, or by sealed ducts.

Fan output was sensed by rakes in the ducting downstream of the fans, but the flow through the fans was not so significant as the flow at the inlets and the exhaust regions. Therefore, to achieve as realistic an airflow as possible at these regions, the duct losses had to be evaluated. This was done by using a plot of fan thrust as measured by the pylon balance versus fan thrust as measured by the pressure rakes in the ducts (see Figure 27).

The Zero Duct Loss line represents the ideal situation: if 100 pounds of thrust were being generated by the fans internally, 100 pounds of thrust would be registered by the pylon balance.

The line for Q = 0.0 represents the actual case with the tunnel shut down; e.g., with the fans generating 100 pounds of thrust, only 56 pounds reach the pylon balance. This can be attributed to blockage caused by having the fan inlets facing machinery which interferes with smooth airflow into their inlets, to friction and turning losses in internal ducting, and to blockage from the internal vanes and deflectors of the exhaust configuration.

As tunnel dynamic pressure built up, the curves shifted to reflect other losses, such as inlet losses brought about by turning the airflow around abruptly curved inlet surfaces, exhaust losses caused by forcing the exhaust to turn to join the external airflow, and by the imposition of turbulent tunnel airflow into the inlet.

The difference between pylon drag at cruise fan power and at the power levels shown on the curve indicated the magnitude of the inlet losses, being the sum of the effects of inlet lip suction, exhaust exit drag, and internal duct losses.

Drag of the Alternate Exhaust Ducts

The data points in Table 8, all taken at zero hub rotation and zero pitch angle, illustrate the effect of the alternative exhaust ducts on overall vehicle drag.

TABLE 8. DRAG OF ALTERNATE EXHAUST DUCTS

Run No.	Fans	Axial Force	Configuration
71	Zero	61.727	Original
75	High	22.039	Original
1012	Zero	47.282	Alternate
1021	High	-22.700	Alternate

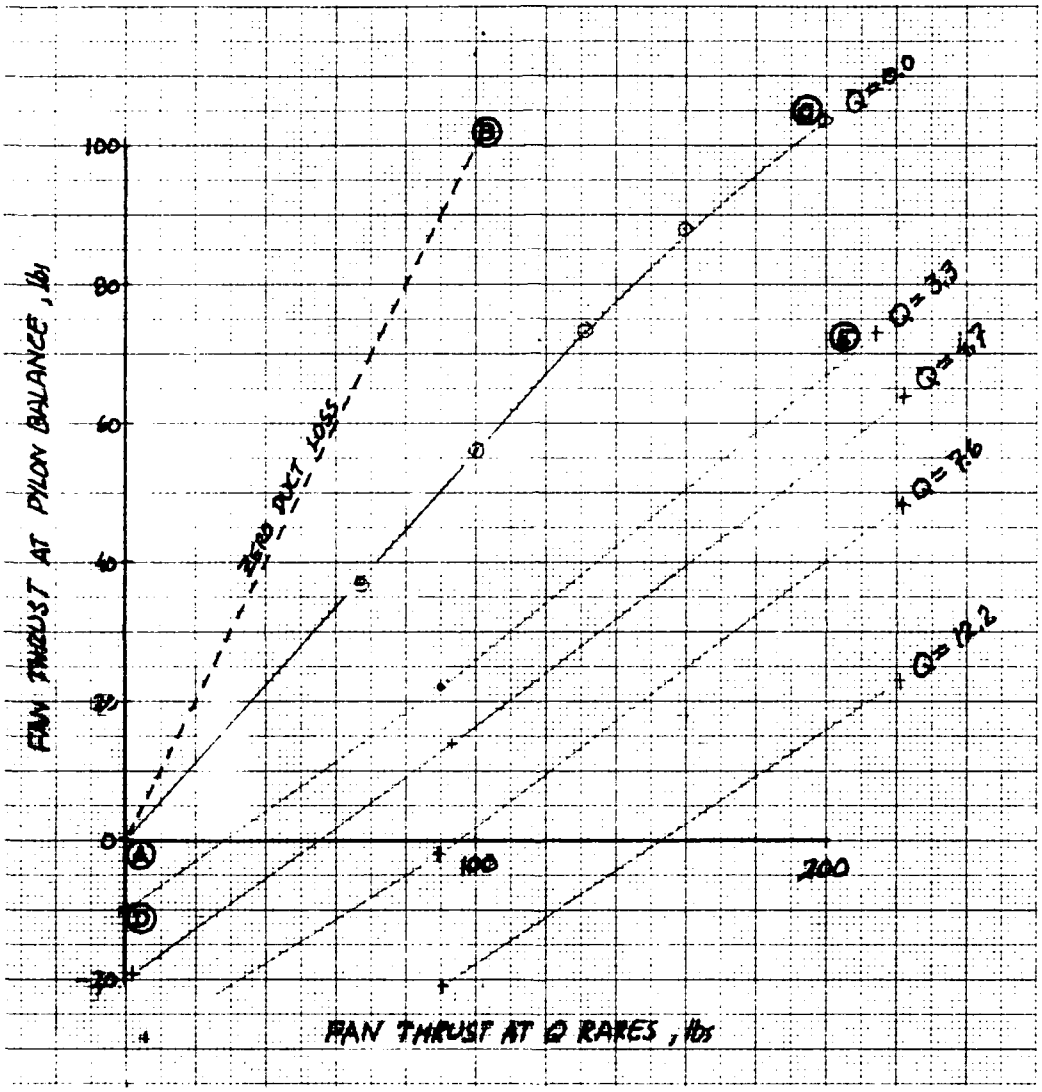

Figure 27. Fan thrust via balance vs pressure rakes.

Under Zero fan conditions, the original configuration yielded 61.727 pounds force at 11.96 psi dynamic pressure, normalized to 12.21 psi dynamic pressure which yields a corrected force of 63.02 pounds. This, compared to 47.282 pounds force shown by the alternate configuration at 12.21 psi dynamic pressure, yields a 15.73-pound reduction in overall vehicle drag, or a 1.28-square-foot drag reduction.

Under High fan conditions, the original configuration yielded 22.039 pounds force at 12.21 psi dynamic pressure, normalized to 12.14 psi dynamic pressure which yields a corrected force of 22.700 pounds. This, compared to -22.831 pounds force shown by the alternate configuration at 12.14 psi dynamic pressure, yields a 44.87-pound reduction in overall vehicle drag, or a 3.67-square-foot drag reduction.

SUMMARY OF FINDINGS

Even though the models were large and heavy, and the balances had large capabilities, operational limitations prevented any overlapping data in "flight" conditions except at very low velocities. This caused the results of the tests to be inconclusive.

BIBLIOGRAPHY

1. Clark, D. R., Dvorak, F. A., Maskew, B., Summa, J. M., and Woodward, F. A., Helicopter Flow Field Analysis, Analytical Methods, Inc., USARTL TR 79-4, Applied Technology Laboratory, U.S. Army Research and Technology Laboratories, Fort Eustis, Virginia, April 1979, AD A069542.

2. Dvorak, F. A., Maskew, B., and Woodward, F. A., Investigation of Three-Dimensional Flow Separation of Fuselage Configurations, Analytical Methods, Inc., USAAMRDL TR 77-4, Applied Technology Laboratory, U.S. Army Research and Technology Laboratories (AVSCOM), Fort Eustis, Virginia, March 1977, AD A039382.

3. Linville, J. C., An Experimental Investigation of the Effects of Rotor Head Configuration and Fuselage Yaw on the Wake Characteristics and Rotor Performance of a 1/8 Scale Helicopter, Sikorsky Aircraft Division, United Technologies Corporation, USAAVLABS TR 69-94, U.S. Army Aviation Materiel Laboratories, Fort Eustis, Virginia, February 1970, AD 869390.

4. Pope, Allen, and Harper, John J., Low Speed Wind Tunnel Testing, John Wiley and Sons, Inc, New York, 1966.

5. Sheehy, T. W., and Clark, D. R., A Method for Predicting Helicopter Hub Drag, Sikorsky Aircraft Division, United Technologies Corporation, USAAMRDL TR 75-48, Eustis Directorate, U.S. Army Air Mobility Research and Development Laboratory, Fort Eustis, Virginia, January 1976, AD A021201.

6. Woodward, F. A., Dvorak, F. A., and Geller, E. W., A Computer Program for Three-Dimensional Lifting Bodies in Subsonic Inviscid Flow, Flow Research, Inc., USAAMRDL TR 74-18, Eustis Directorate, U.S. Army Air Mobility Research and Development Laboratory, Fort Eustis, Virginia, April 1977, AD 782202.

END
DATE
FILMED
9-88
DTIC